NO_x Reduction from Diesel Emissions over a Nontransition Metal Zeolite Catalyst: A Mechanistic Study Using FTIR Spectroscopy

Young Hoon Yeom, Bin Wen,† Wolfgang M. H. Sachtler,† and Eric Weitz*

Institute for Environmental Catalysis and Department of Chemistry, Northwestern University, Evanston, Illinois 60208

Received: November 17, 2003; In Final Form: January 21, 2004

The reactions of acetaldehyde, acetic acid, and nitromethane with NO_2 on a BaNa−Y zeolite are monitored with FTIR spectroscopy, typically at 473 K. Isotopic labeling was used to help elucidate reaction pathways and intermediates. The mechanism that has been deduced for the reaction of NO_2 with acetaldehyde starts with the formation of acetate ions and subsequently the aci-anion of nitromethane. NO_2 can react with the aci-anion of nitromethane, which is stabilized in the ionic environment of the zeolite to form a proposed $O_2NCH_2NO_2^-$ intermediate. At 473 K, the $O_2NCH_2NO_2^-$ intermediate is expected to swiftly lose NO_2 and H_2O yielding the formonitrile oxide anion, CNO^-, which can isomerize to NCO^- and react with a proton to form HNCO. The formation of an $O_2NCH_2NO_2^-$ intermediate is consistent with the observation of both isotopomers of HNCO when $^{15}NO_2$ is a reactant. Also, as expected for an $O_2NCH_2NO_2^-$ intermediate, all four isotopomers of N_2O are observed. In the next step, NH_3 and CO_2 are formed from HNCO + H_2O. Thus, in this system ammonia is formed by the sequence: $CH_3CHO \rightarrow CH_3COO^- \rightarrow CH_2NO_2^- \rightarrow O_2NCH_2NO_2^- \rightarrow CNO^- \rightarrow HNCO \rightarrow NH_3$. NO_2 is the reaction partner in the first three steps; a proton is added in the fifth step and H_2O is the co-reactant in step 6. Once NH_3 is formed, well-known chemistry can lead to the formation of N_2. Remarkably, in this system N_2 formation as a result of reduction of NO_x occurs in the absence of a transition metal. The formation of nitromethane is observed when acetaldehyde reacts with NO_2. When added nitromethane reacts with $^{15}NO_2$, formation of $^{14}NO_2$ is observed, which is also consistent with formation of an $O_2NCH_2NO_2^-$ intermediate. The reaction channel outlined above is also followed by acetic acid and results in a very high CO_2/CO ratio (>20:1). The reaction of either acetic acid or acetaldehyde with NO_2 gives a similar set of products, except that the CO to CO_2 ratio is higher *and* methanol is formed when acetaldehyde is the reactant. These observations suggest that a parallel reaction channel exists for acetaldehyde which could involve free radicals. Such a path would likely be initiated by NO_2 abstracting a H atom from acetaldehyde. One possible reaction path for the resulting acetyl radical is dissociation to CO and a methyl radical. Gas-phase nitromethane is also observed with acetaldehyde but not with acetic acid as the reactant. Nitromethane could come from neutralization of an ionic precursor or it could be a product of the additional reaction channel for acetaldehyde alluded to above.

I. Introduction

The research described in this paper is motivated by a combination of two incentives. First, there is a societal necessity to abate toxic nitrogen oxides in the emissions from highly fuel-efficient diesel engines. To develop superior catalysts for this process, a better understanding of the relevant chemistry is required. A second, purely scientific incentive arises from the discovery that the reduction of nitrogen oxides over zeolite catalysts does not require a transition metal. How this occurs is an interesting and significant scientific issue.

For automotive applications, it would be desirable to place a highly active and selective catalyst in the exhaust system of a diesel powered car or truck. This catalyst should have the ability to securely transform all nitrogen oxides, subsequently called NO_x, into environmentally benign molecules. It should operate at the relatively low temperature of diesel emission gases, preferentially even under cold start conditions. It should destroy NO_x completely at realistic gas velocities in the presence of H_2O and O_2, which are present in concentrations far exceeding the few hundred ppm of NO_x. The ideal catalyst should retain this ability for the life of the vehicle. If an additive is used to chemically reduce NO_x, that reductant should be safe, cheap, and only negligibly affect the fuel efficiency of the diesel engine. Although legislation to strongly reduce the NO_x content in diesel emissions is pending in many countries, no catalyst is presently known that can efficiently perform this task.

Some zeolite-based materials have been identified that catalyze NO_x reduction with hydrocarbons in the presence of a large excess of H_2O and O_2, but these materials require a higher temperature (~623 K) than desirable for diesel exhaust gas (~473 K).[1] Ammonia, which can be produced on board from an aqueous solution of urea, has the advantage over hydrocarbons that it is effective at NO_x removal at lower temperatures.[2,3] However, care must be taken in controlling the introduction of ammonia since any unconverted ammonia is easily oxidized, giving more NO_x.

The reduction of NO or NO_2 to N_2 by any molecule implies an oxidation of that molecule. Partial or total oxidation of organic molecules is at the base of numerous industrial processes

* Address correspondence to this author. E-mail: weitz@northwestern.edu.
† Also Center for Surface Science and Catalysis.

10.1021/jp037504e CCC: $27.50
Published on Web 04/03/2004

and many of the relevant mechanisms for these processes have been studied in considerable detail.[4] Conversion of propene to acrolein[5] or acrylonitrile,[6] production of maleic acid anhydride from either benzene or butane, and conversion of xylenes to terephthalic acid are well-known examples of important industrial oxidation processes which are catalyzed by transition-metal oxides.[4]

Mechanistic studies have revealed that C−H bonds are usually broken in a cascade of successive steps in which a transition-metal ion is reduced to a lower oxidation state. Subsequent capture of oxygen from the gas phase will reoxidize the transition-metal ion to its original state. The mechanism originally proposed by Mars and van Krevelen describes this scenario in detail.[7]

However, for the oxidation of organic molecules by NO_x over a zeolite-based "deNO_x catalyst", the rules of the game appear to be quite different from those of the Mars−van Krevelen mechanism. Iwamoto was the first to show that reduction of NO over Cu/MFI starts with the oxidation of that molecule to NO_2.[8,9] Work by Chen et al. with Fe/MFI catalysts demonstrates that reaction of NO_2 with *iso*-butane leads to the formation of a deposit which appears to contain amine groups. Using isotopic labeling, these authors showed that N_2 molecules are predominantly formed by the chemical interaction of gaseous NO_x with these amine groups.[10,11] This chemistry was studied in more detail by Sun et al.[3,12] who used labeled NH_3. Their results proved that the N_2 molecules that are formed on an Fe/MFI catalyst are 100% heteronuclear, that is, one N atom came from NO, the other from NH_3. Moreover, the oxygen consumption is exactly equal to that required to convert NO to N_2O_3. As N_2O_3 is in kinetic equilibrium with NO + NO_2, and since it forms HONO on reaction with water, the authors conclude that adsorbed ammonium nitrite, NH_4NO_2, is the cradle from which the N_2 molecule is born:

$$O + NO_2 \rightarrow N_2O_3 \quad (1)$$

$$N_2O_3 + H_2O \rightarrow 2HONO \quad (2)$$

$$HONO + NH_3 \rightarrow NH_4NO_2 \rightarrow N_2 + 2H_2O \quad (3)$$

It has been known for over a century[13] that at temperatures only somewhat above room-temperature ammonium nitrite decomposes to yield diatomic nitrogen.

In summary, the classical Mars−van Krevelen mechanism assumes a cascade of oxidation steps of an organic molecule in which a transition-metal ion oscillates between two oxidation states. By contrast, the N atom in NO_x starts from an oxidation state, $N_{ox} = +2$, becomes +3 in HONO, and +4 in NO_2. When interacting with an organic molecule, it is reduced to $N_{ox} = -3$. This nitrogen species can interact with a nitrogen atom in oxidation state +3 to form N_2. In some circumstances, these steps might not require a transition-metal ion, but simply exploit the ability of nitrogen to change its oxidation state in processes such as the Beckmann rearrangement of oximes to amides or the conversion of nitromethane to CO_2 + NH_3, for example, via an isocyanic acid intermediate. Indeed, Satsuma et al. showed[14] that over a zeolite catalyst nitromethane is converted to CO_2 + NH_3, and after partial deactivation of the catalyst, isocyanic acid was detected by IR spectroscopy. They also obtained evidence for isocyanic acid's cyclic trimer, cyanuric acid, and found that melamin was formed upon exposure of the system to ammonia.

In light of these considerations, it is very interesting that Peden et al.[15] recently reported that acetaldehyde reduces NO_x to N_2 over NaY or BaY catalysts *in the absence* of a transition metal. In a previous paper,[16] we confirmed this finding with BaNa−Y and showed that a small Fe impurity in the Y zeolite is of no relevance for this process, if treatments are avoided that will transport the Fe ions from zeolite lattice tetrahedra to exchange positions. We also showed that 90% conversion to N_2 was achieved at 473 K and a space velocity of 30 000 h^{-1} with NO_x containing a NO_2/NO ratio exceeding unity.

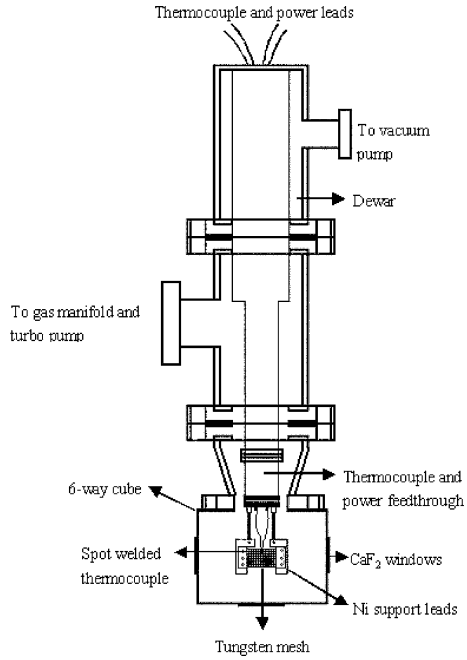

Figure 1. High vacuum variable temperature infrared cell with liquid-nitrogen cooling capabilities.

In this paper, we report FTIR and time-resolved (rapid scan) FTIR studies of the chemistry of acetaldehyde on BaNa−Y zeolite. We have focused on the interaction of acetaldehyde with NO_2 and an elucidation of the mechanism involved in the formation of N_2 from these species. We also report data on the chemistry of acetic acid and nitromethane on BaNa−Y in the presence of NO_2.

II. Experimental Section

Our zeolite sample was obtained by a threefold wet ion exchange of Na−Y (Si/Al = 2.5, Aldrich) with a 0.1 M $Ba(NO_3)_2$ solution at ambient temperature. For every exchange, the slurry was stirred for 48 h prior to being vacuum filtered, washed thoroughly with doubly deionized H_2O, and dried in air. Elemental analysis via inductively coupled plasma spectroscopy (ICP) gave the following unit cell composition: $Ba_{9.6}Na_{33.8}Al_{53}Si_{139}O_{384}\cdot xH_2O$. Evidence has been presented to show that this zeolite acts functionally like a Ba−Y zeolite.[15] However, since there is a higher Na^+ than Ba^{2+} concentration, we will refer to the sample as a BaNa−Y zeolite.

In-situ FTIR spectra were recorded with a Bio-Rad Excalibur FTS-3000 infrared spectrometer equipped with a MCT detector. Unless otherwise stated, each spectrum was obtained by averaging 50 scans at a resolution of 2 cm^{-1}. The "homemade" infrared cell is based on the design in ref 17 and consists of a stainless steel cube with two CaF_2 windows that can be differentially pumped. A schematic of the cell design is given in Figure 1. The tungsten grid, which supports the sample, is held in place by Ni jaws and can be resistively heated to a temperature that is measured by a Chromel−Alumel thermocouple spot-welded to the center of the grid. The nickel jaws

are attached to the copper rods of a power/thermocouple feedthrough that is welded to the bottom of a stainless steel Dewar that can hold a cryogenic fluid for sample cooling.

Typically, 10−15 mg of zeolite in a water slurry were "painted" onto the 1.5 × 1.5 cm tungsten grid, using a small brush, while the grid was held at 353 K. The IR cell was then evacuated to a pressure of 5×10^{-7} Torr by a turbomolecular pump. The zeolites samples were heated under vacuum to 753 K and were kept at that temperature for 10 h to remove adsorbed water. A fresh zeolite sample was used for each new set of experiments. These samples were used to obtain FTIR spectra of the zeolite films in a transmission mode. In some experiments, 50 mg of zeolite sample was painted onto the tungsten grid. This was done in experiments in which it was desirable to increase the yield of gas-phase products. However, this amount of zeolite resulted in films that were essentially opaque to IR radiation.

Gas mixtures of NO + O_2 were prepared at room temperature and allowed to react for a suitable time (typically overnight) such that the NO and NO_2 in the mixture are assumed to be in equilibrium, which means that virtually all the NO was converted to NO_2. This procedure, which generated what will be referred to as a "premix," was generally used in these studies in preference to starting with just NO_2 or mixtures of NO_2 + O_2 since, when desired, labeled ^{15}N from ^{15}NO could be incorporated into the NO_2 without changing the reaction protocol.

The following procedure was used to determine the number of acetaldehyde or acetic acid molecules that were adsorbed into the BaNa−Y zeolite. A 5 L bulb that was filled with either 2 Torr of acetaldehyde or 2 Torr of acetic acid was attached to the IR cell. The compound in the bulb was introduced into the IR cell in which the sample was held at 473 K. The valve on the bulb was allowed to stay open until the "equilibrium" pressure of 1.2 Torr for acetaldehyde and 0.4 Torr for acetic acid was established. At that point the valve to the cell was closed, and the remaining amount of gas in the bulb was determined by measuring its pressure at room temperature. Taking into account the volume of the cell and vacuum system, the number of adsorbed molecules could be determined. Assuming that all adsorbed molecules reside in the supercages of BaNa−Y leads to a determination that each supercage of BaNa−Y has 0.9 acetaldehyde and 3.0 acetic acid molecules at 473 K when the zeolite is in contact with the gas-phase equilibrium pressures noted.

To probe whether surface nitrate species are displaced by acetate, a premade mixture of 1 Torr of NO and 50 Torr of O_2 is introduced into BaNa−Y at 320 K. Thus, in the absence of any adsorption the cell pressure would be 51 Torr. After the NO_2 has an opportunity to adsorb into the BaNa−Y, the integrated absorbance of the remaining gas-phase NO_2 (at 1616 cm^{-1}) is recorded. Subsequently, the cell was evacuated at 703 K for 10 h to effectively remove all of the surface nitrate. After this procedure, a premix of 1 Torr of acetic acid + 1 Torr of NO + 50 Torr of O_2 is introduced into the cell at 320 K. After the mixture has an opportunity to adsorb, the integrated absorbance of the remaining gas-phase NO_2, at 1616 cm^{-1}, is again recorded, yielding a higher gas-phase NO_2 concentration with the acetic acid mixture than with the mixture containing just NO + O_2. On the basis of these experiments, there is ∼53% less adsorbed surface nitrate after the sample has been exposed to the indicated acetic acid mixture.

Similar experiments were conducted in the presence of water at 373 K. The same procedures were used except that the premixes contained 2 Torr of H_2O + 2 Torr of NO + 100 Torr of O_2 or 2 Torr of H_2O + 2 Torr of NO + 2 Torr of acetic acid + 100 Torr of O_2. On the basis of these experiments, there is ∼50% less adsorbed surface nitrate when the sample has been exposed to the acetic acid mixture in the presence of H_2O.

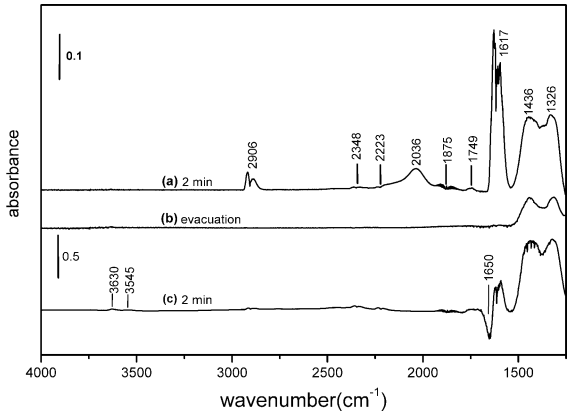

Figure 2. FTIR spectra observed upon exposing BaNa−Y to 2 Torr of NO and 100 Torr of O_2 at 473 K (a) after 2 min, (b) after subsequent evacuation, and (c) after BaNa−Y is preexposed to 10 Torr of H_2O before exposure to the premix.

Acetaldehyde (Aldrich, 99.5%), acetic acid (Supelco, 99%), acetic acid-1-^{13}C (Aldrich, 99% ^{13}C), acetic acid-2-^{13}C (Cambridge Isotope, 99% ^{13}C), crotonaldehyde (Fluka, 98%), nitric oxide (Matheson Tri-Gas, 99%), nitric oxide-^{15}N (Cambridge Isotope, 98% ^{15}N), nitromethane (Aldrich, 99%), nitromethane-d_3 (Aldrich, 99%), and nitromethane-^{13}C (Aldrich, 99% ^{13}C) were used as received.

III. Results and Band Assignments

A. Adsorption of NO + O_2. NO readily reacts with O_2 in the gas phase to give NO_2, which can further dimerize to N_2O_4. The facile dimerization of NO_2 to N_2O_4 is attributed to the unpaired electron in NO_2, which is preferentially localized on the N atom.[18] It is known that N_2O_4 can disproportionate to NO^+ and NO_3^- on a MnO_2/Na−Y composite at room temperature, where NO^+ interacts with surface oxygen $(O^{2-})_{surface}$ and NO_3^- interacts with the Na^+ ions.[19]

When dehydrated BaNa−Y is exposed to a premixture of NO and O_2 at 473 K, strong absorptions are immediately observed at 1326 and 1436 cm^{-1}. These are due to the symmetric and asymmetric vibrations[20] of NO_3^- interacting with Ba^{2+} ions (see Figure 2). The corresponding surface nitrate species formed but were much less prominent for Na−Y at 473 K (not shown). Analogous to what has been observed in the MnO_2/Na−Y system,[19] the main route to the formation of the NO_3^- in the absence of H_2O on BaNa−Y is expected to be

$$2NO_2 \rightarrow N_2O_4 \rightarrow NO^+ + NO_3^- \qquad (4)$$

A weak feature is seen at 1749 cm^{-1}. This absorption is in a region where the asymmetric stretching modes of N_2O_4[21] could absorb along with the $\nu_1 + \nu_4$ combination vibration of NO_3^- ions.[22] Since high temperature does not favor the formation of N_2O_4 (vida infra), and it is clear that NO_3^- ions are present, it is likely that this absorption is primarily due to the $\nu_1 + \nu_4$ combination vibration of NO_3^- ions. Absorptions centered at 1617 and 2906 cm^{-1} are due to gas-phase NO_2 and the weak absorptions centered at 2223 and 2348 cm^{-1} are due to N_2O and CO_2 which are both present as impurities in the NO used to make the premix.[23] The absorption of gas-phase NO is seen at 1875 cm^{-1}.

A band at 2036 cm^{-1}, which is due to NO^+ (spectrum a),[19,20,24] appears immediately after exposure of BaNa−Y to the NO + O_2 premix and slowly decreases in intensity over several hours (data for the entire time scale of the experiment are not presented). Similar behavior and features have recently been reported when Na−Y is exposed to NO_2.[22] As discussed below, NO^+ rapidly disappears in the presence of water. The NO^+ band is not observed in the presence of preadsorbed H_2O and instantaneously and completely vanishes as a result of adding H_2O to a BaNa−Y sample in which it is observed. We assign the reaction involved to

$$NO^+ + NO_2 + H_2O \rightarrow 2H^+ + NO_3^- + NO \qquad (5)$$

This assignment is supported by the growth of a band at 3630 and 3545 cm^{-1} because of H^+, which is not seen when dehydrated BaNa−Y is simply exposed to water. Thus, the observed slow disappearance of the NO^+ absorption in the absence of added water, that is alluded to above, could be due to reaction of NO^+ with small quantities of H_2O desorbed from the walls of the IR cell.

The stretching vibration of NO^+ is shifted to higher wavenumbers relative to NO because of shortening of the NO bond as a result of loss of an electron from the π^* orbital. The isotopic shift of $^{15}NO^+$ on BaNa−Y is 34 cm^{-1}(not shown), which is in good agreement with literature values,[24,25] thus supporting our assignment. In these studies, NO^+ was observed on Na−Y at 298 K (not shown) but not at 473 K suggesting that the interaction energy of NO^+ with the framework oxygens in Na−Y is weaker than the corresponding interaction in BaNa−Y.

Evacuation of a cell containing BaNa−Y that has been predosed with NO_2 and thus exhibits surface nitrate absorptions, for 10 min at 473 K, leads to the loss of ∼80% of the amplitude of these absorptions. Since the back reaction of eq 4 leads to formation of a gas-phase species which can be removed by evacuation, we believe the reverse of reaction 4 is responsible for loss of amplitude of the nitrate absorption when the cell is evacuated. NO^+ is completely removed by the same treatment (see spectrum b). The fact that some nitrate remains on the surface implies that there are different sites that nitrate can interact with, and one set of these sites leads to stronger interactions. It is also possible that nitrate is formed by two or more different mechanisms which populate different sites.

Since the NO^+ band completely disappears upon evacuation of the cell, the remaining nitrate must have a different counterion. There are indications in the literature that reactions 6 and/or 7 could participate in nitrate formation.[20,21,26−28]

$$3NO_2 + H_2O \rightarrow 2NO_3^- + 2H^+ + NO \qquad (6)$$

$$OH + NO_2 \rightarrow NO_3^- + H^+ \qquad (7)$$

Reaction 6 requires water and thus could be more significant in the presence of H_2O. In spectrum c, where the BaNa−Y has been predosed with water prior to exposure to NO + O_2, there are absorptions at 3630 and 3545 cm^{-1} which do not appear or are negligible in spectrum a. In addition, the NO^+ absorption is not observed. The appearance of these bands and the production of H^+ ions via reaction 6 are consistent with the negative feature at 1650 cm^{-1} in spectrum c. As the predosed sample is the background for spectrum c, a "negative feature" indicates rapid depletion of water upon introducing the NO + O_2 premix. We assign this process to reaction 6. The very low intensity of the 3630 cm^{-1} absorption in spectrum b is due to Brønsted acid sites formed by reactions 5 and/or 6 where NO_2 reacts with what are presumably small quantities of H_2O that are desorbed from the cell walls. Additionally, when water is preadsorbed on the BaNa−Y sample, there is less nitrate that is readily removable via evacuation. This result is consistent with the idea that reactions 5 and 6 lead to a more strongly bound nitrate species.

The concentration of the Brønsted acid sites in our samples of dehydrated BaNa−Y must be quite low since there is no absorption at ∼3600 cm^{-1} either before or immediately after introducing the NO+O_2 premix (spectrum a). A negative feature would have appeared in the 3600 cm^{-1} region of spectrum a if these sites had interacted with NO_2 (reaction 6). This reaction would be expected to produce HNO_3 which would then be expected to produce a surface NO_3^- along with a H^+. There was no evidence for such reactions despite the fact that there is ample literature evidence to indicate that NO_2 will react with Brønsted acid sites if they are present.[20] The lack of evidence for a reaction of NO_2 with Brønsted acid sites, coupled with the absence of a negative feature in the 3600 cm^{-1} region of spectrum a, implies a minimal concentration of Brønsted acid sites in our zeolite sample.

It has been reported that there is one acidic site per ∼116 Al atoms in alkali metal-exchanged Y zeolites but none in pure defect-free Ba−Y.[29] The small concentrations of Brønsted acid sites present in most commercial zeolite Y samples are thought to result from cation deficiencies caused by the replacement of M^+ by H_3O^+ during ion exchange in the synthesis of the zeolites and by incomplete dehydration.

Nitrites are also plausible surface species that could form by the reaction of NO^+ with $(O^{2-})_{surface}$ which in turn could form from reaction 4 upon introducing the NO + O_2 premix to zeolite Y.[19,20] In fact, surface nitrite species have been reported to form on exposure of Ba−Y to NO_2 at 323 K.[20] No nitrite was detected on BaNa−Y at 1330 cm^{-1} in the present work at 473 K, presumably because of the instability[20] of surface nitrite at this elevated temperature. However, we have observed surface nitrite bands near room temperature (not shown).

As mentioned previously, the infrared absorption intensity of the NO_3^- bands on BaNa−Y at 473 K is much larger than with Na−Y. Literature data indicate that Ba−Y shows higher catalytic activity for NO_x reduction than Na−Y.[15] A greater capacity for "storage" of NO_x species by Ba−Y may be one of the factors explaining this difference in catalytic activity. Alkali and alkaline earth metal-exchanged Y zeolites and supported alkali and alkaline earth metal oxides have been identified as promising materials for NO_x traps.[20,28,30] Monticelli et al. have studied NO_x adsorption−desorption behavior on alkali and alkaline earth metal-exchanged Y zeolites, including Ba−Y, and they found that NO_2 is selectively adsorbed, while NO is inert to these adsorbents.[28] They also report a correlation between the exchanged cation and the NO_x storage capacity (Ba−Y > Cs−Y > Na−Y > Li−Y) and indicate that ∼1.7 NO_x molecules per supercage of Ba−Y, which has three Ba^{2+} ions per supercage, are adsorbed at 403 K in the presence of water. Prinetto et al. have studied the NO_x storage properties of BaO/Al_2O_3 and Pt−BaO/Al_2O_3 catalysts with FTIR and TPD.[31] They found that the presence of barium increases both the amount of the stored NO_x and its thermal stability.

B. Adsorption of Acetic Acid and Acetaldehyde. Figure 3 shows a portion of the FTIR spectra obtained after introducing acetic acid (panel a) and acetaldehyde (panel b) into BaNa−Y at 473 K. As seen in panel a, when BaNa−Y is exposed to 0.4 Torr of acetic acid, absorptions appear at 1308, 1332, 1384,

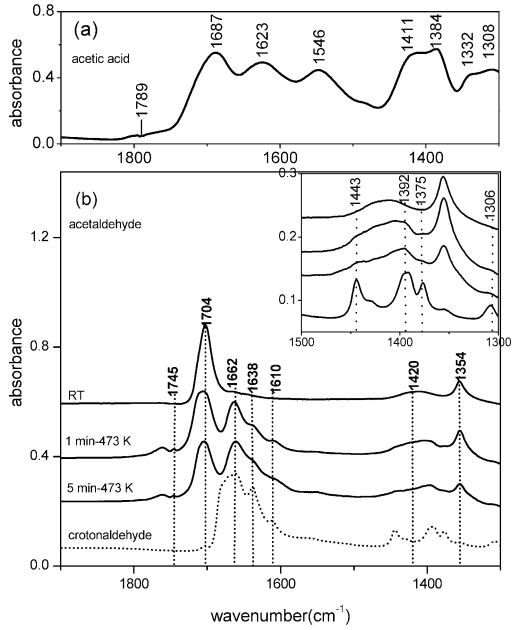

Figure 3. FTIR spectra observed upon exposing dehydrated BaNa−Y to (a) 0.4 Torr of acetic acid for 5 min. (b) From top to bottom: BaNa−Y was exposed to 1.2 Torr of acetaldehyde at 298 K for 5 min, and then the cell was evacuated. In the next spectrum, BaNa−Y was exposed to 1.2 Torr of acetaldehyde at 473 K for 1 min. The subsequent spectrum is for exposure at 473 K for 5 min. In the bottom spectrum, BaNa−Y is exposed to 0.3 Torr of crotonaldehyde for 5 min. The insert shows an expansion of the 1300−1500 cm^{-1} region.

1411, 1546, 1623, 1687, and 1789 cm^{-1}. Though there is some controversy regarding the assignment of specific vibrational normal modes to these absorption bands, it is clear that there is a close qualitative correspondence between the spectrum of acetic acid on MgO and the spectrum in Figure 3.[32] The band at 1789 cm^{-1} is due to gas-phase acetic acid. This band corresponding to gas-phase acetic acid was eliminated by evacuation at 473 K for 10 min. The bands corresponding to adsorbed acetic acid were slightly reduced in intensity by this procedure.

The top spectrum in Figure 3, panel b, was obtained by exposing BaNa−Y to 1.2 Torr of acetaldehyde for ∼5 min at 298 K and then evacuating for 10 min. The major absorptions of acetaldehyde seen in Figure 3b are at 1354 (δ_s CH_3), 1420 (broad) (δ CH and δ_{as} CH_3), 1704 (ν CO), 2769 (ν CH), 2873 (ν_σ CH), and 2913 cm^{-1} (ν_{as} CH_3). The last three absorptions are not shown in Figure 3. The vibrational assignments for these bands are based on analogies to data for acetaldehyde in the gas phase and in a CoAlPO-5 zeolite.[33,34] The second and third spectra were obtained by exposing BaNa−Y to 1.2 Torr acetaldehyde at 473 K for 1 and 5 min, respectively. New absorption bands, which are not observed in the top spectrum, which was obtained at 298 K, immediately emerged at the following frequencies: a shoulder at 1306 (see inset), 1375, 1392 (broad), 1443 (broad), 1610, 1638, and 1662 cm^{-1}.

The absorption centered at 1745 cm^{-1} is due to gas-phase acetaldehyde.[35] The pattern of these new absorptions is very similar to what is seen in the bottom spectrum, which was obtained by exposing BaNa−Y to 0.3 Torr of authentic crotonaldehyde at 298 K for 5 min. Identification of new absorptions in the C−H stretching region (not shown) was difficult because product bands overlap with acetaldehyde absorptions. The band at 1662 cm^{-1} is assigned to a C═O stretch of crotonaldehyde interacting with Ba^{2+} and the 1638 cm^{-1} absorption is assigned to a C═C stretching mode of crotonaldehyde. The feature at 1610 cm^{-1} is assigned to a C═C stretch of crotonaldehyde interacting with Ba^{2+}. Bands at 1375 and 1443 cm^{-1} are due to the symmetric and asymmetric deformations of the methyl group in crotonaldehyde.[36] The 1392 cm^{-1} band corresponds to a C−H bending mode.[33] The assignment of the 1306 cm^{-1} band is less certain but may correspond to a CH═ in-plane deformation of crotonaldehyde.[36]

Crotonaldehyde is rapidly formed from acetaldehyde on BaNa−Y at 473 K via an aldol condensation reaction:

$$2\ \text{acetaldehyde} \rightarrow \text{crotonaldehyde} + \text{water}$$

which will be described in more detail in section IV. C.

On BaNa−Y, the carbonyl group vibrations of both acetaldehyde and acetic acid are shifted more strongly to lower wavenumbers than the corresponding vibrations on Na−Y (not shown). On the basis of the shifts of the band positions of acetaldehyde and acetic acid, these molecules preferentially interact with Ba^{2+} ions which, as discussed below, are probably located at site II. (The definition of the cation sites of faujasite type zeolites is provided in ref 37.)

It has been reported that charge-compensating divalent cations in zeolite Y have a tendency to move from sites I and I′ to supercages (site II) when the cations are exposed to guest molecules, like H_2O (in NiNa−Y)[38] and CO_2 (in BaNa−Y).[39] By the same reasoning, it is plausible that Ba^{2+} ions move into site II to associate with acetaldehyde and acetic acid molecules. The absence of a Na^+ ion contribution to the infrared spectrum of acetaldehyde on BaNa−Y can be understood on the basis of the following reasoning. There are 9.6 Ba^{2+} ions per unit cell in our samples, and each supercage is occupied by 1.2 Ba^{2+} ions, if the ions preferentially occupy site II. On the basis of our measurement of adsorption, each supercage of BaNa−Y should have an average of 0.9 acetaldehyde molecules at 473 K at the equilibrium pressure of 1.2 Torr. Thus, at this loading, on the basis of these averages, acetaldehyde molecules would be expected to preferentially interact with Ba^{2+} ions since the interaction between the cation and adsorbed acetaldehyde is stronger with Ba^{2+} than with Na^+. However, at least superficially, acetic acid, with a calculated average of 3.0 acetic acid molecule per supercage at an equilibrium vapor pressure of 0.4 Torr would be expected to saturate the Ba^{2+} sites.

Though one of the intermediates that is observed (at 2255 cm^{-1}) is seen on both BaNa−Y and Na−Y at 473 K, the other surface-bound intermediates are only seen on BaNa−Y (vida infra). Thus, clearly the interaction of surface species with Ba ions dominates over the interaction with Na^+ ions. The explanation for this with acetaldehyde can simply be ascribed to the ratio between acetaldehyde molecules and Ba^{2+} ions. The explanation is less definitive for acetic acid. However, it is possible that the ICP procedure used to obtain the number of Ba^{2+} ions underestimates the actual number, or perhaps more likely, acetic acid condenses on the surface of the BaNa−Y zeolite or the metal surfaces of the IR cell. However, independent of the explanation, it is clear that the intermediates we observe are present in higher concentration on BaNa−Y than on Na−Y. This trend parallels the higher activity of BaNa−Y for deNO_x reactions.

C. Reaction of Acetaldehyde with the NO + O_2 Premix. Figure 4 displays rapid-scan spectra taken to further probe the reactions of acetaldehyde on BaNa−Y. These spectra had an acquisition time of 1 s at 4 cm^{-1} resolution. The reactants: 1.4 Torr of acetaldehyde, 1.5 Torr of NO, and 100 Torr of O_2 were premixed before being introduced into the cell which contained the BaNa−Y sample. The premix is allowed to stand for a

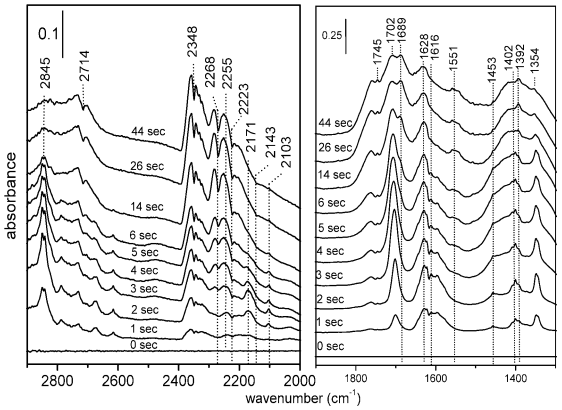

Figure 4. Time-resolved FTIR spectra taken after exposure of BaNa−Y to a premixed gas mixture of 1.4 Torr of acetaldehyde, 1.5 Torr of NO, and 100 Torr of O_2 at 473 K. The exposure time is indicated for each spectrum.

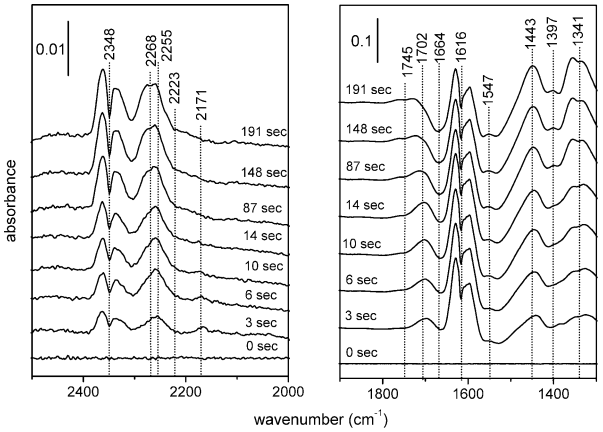

Figure 5. Time-resolved FTIR spectra taken after exposure of BaNa−Y, which was preexposed to 0.4 Torr of acetic acid, to a premix of 1.8 Torr of NO and 100 Torr of O_2 at 473 K. The reaction time is indicated on each spectrum.

sufficient time that reaction between NO and O_2 leads to the major NO_x species present being NO_2. The formation of NO_2 from NO + O_2 is exothermic by 13.64 kcal/mol, formation of N_2O_4 from NO_2 is exothermic by 20.52 kcal/mol. ($K = 2.26 \times 10^{12}$ atm^{-1} for $2NO + O_2 \rightarrow 2NO_2$ and 1.43×10^{-1} atm for $N_2O_4 \rightarrow 2\ NO_2$ at 294 K.)[40]

The reactant mixture was introduced into the infrared cell by manually opening a butterfly valve while the rapid scan software was running. Upon introducing the acetaldehyde + NO + O_2 premix, absorption bands immediately appear at 1354 and 1702 cm^{-1} which are indicative of adsorbed acetaldehyde. The increase in intensity of the adsorbed acetaldehyde between 1 and 3 s is due to the finite time required for acetaldehyde introduced into the cell to reach the zeolite sample and adsorb. The intensity of the acetaldehyde absorptions gradually decreases with increasing exposure time.

There is no measurable reaction on the experimental time scale for acetaldehyde in the gas phase with either NO or O_2 alone, or with NO_2 or on BaNa−Y with either NO or O_2 alone. Thus, it is clear that the decrease in acetaldehyde on exposure to BaNa−Y is the result of a reaction of adsorbed acetaldehyde with NO_2 formed in the premix. The fact that NO_2 consumption at 1616 cm^{-1} parallels acetaldehyde loss (Figure 4) also indicates that a reaction is taking place.

Absorption bands appear at 1745 and 2714 cm^{-1} which are known absorptions of gas-phase acetaldehyde. These bands increase in intensity over the time scale of the experiment. (The baseline for these spectra corresponds to the $t = 0$ spectrum.) Though this behavior could be due to desorption, we have demonstrated in separate experiments that both the 1745 and 2714 cm^{-1} bands of gas-phase acetaldehyde increase in intensity as the temperature of gas-phase acetaldehyde increases. These changes could be due to a temperature-dependent gas-phase equilibria between acetaldehyde and it oligomers. Thus, the observed growth in intensity of these bands may simply be a consequence of an increase in the temperature of the gas-phase sample as it is heated by the wire grid and holder.

Both gas-phase acetaldehyde and formaldehyde absorb at 1745 cm^{-1}. It is clear that this band has a contribution from acetaldehyde, since the peak at 2714 cm^{-1} is due to gas-phase acetaldehyde and has similar kinetics to that observed for the 1745 cm^{-1} absorption. However, a contribution to the 1745 cm^{-1} from formaldehyde, which corresponds to the strongest band of gas-phase formaldehyde, cannot be excluded.[23] In separate experiments, when formaldehyde is introduced into the cell without any potential reactants, the center of an absorption band (taken at 2 cm^{-1} resolution) is readily observable at 1744.4 cm^{-1}. In addition, there is a weak absorption at 1745 cm^{-1} when acetic acid is the reductant (see Figure 5 below) and it is difficult to construct a plausible scheme that results in the production of acetaldehyde from acetic acid via reaction with NO_2. Thus, we believe that formaldehyde is also present in the gas phase.

The absorption at 1616 cm^{-1}, which is due to gas-phase NO_2, is barely visible after 26 s, because NO_2 is consumed by reaction with acetaldehyde and subsequent reaction intermediates. While NO_2 is being consumed, four bands at 1392, 1551, 1628, and 1689 cm^{-1} increase in intensity. The positions of these bands and their relative intensities are in good agreement with the positions and intensities of absorptions of acetic acid adsorbed on BaNa−Y (see panel a in Figure 3).[32] These acetate bands are visible even after 44 s because the concentration of NO_2 was so low that all of it was consumed during this time period. When the zeolite was dosed with 2.4 Torr of NO_2, acetate absorptions were only observed for a few seconds (not shown). The absorption with multiple low intensity peaks in the 1500 cm^{-1} region, which can be seen in the spectra taken after 14 s, is due to the gas-phase H_2O product of the reaction of acetaldehyde with NO_2.

As seen in Figure 4, there is a dramatic change in the region between 2000 and 2500 cm^{-1} as a function of reaction time. Three gas-phase bands centered at 2143 (weak), 2223, and 2348 cm^{-1} grow as a function of reaction time. The 2143 and 2348 cm^{-1} absorptions are readily assigned to gas-phase CO and CO_2, and the 2223 cm^{-1} absorption is assigned to gas-phase N_2O, which is present as an impurity in the NO reactant. However, N_2O is also produced by the reaction between acetaldehyde and NO_2, as evidenced by the fact that the relevant absorption grows in intensity as the reaction progresses.

Four bands due to intermediates are present at 2103, 2171, 2255, and 2268 cm^{-1}. Interestingly, the two intermediate species at 2103 and 2171 cm^{-1} were not detected with Na−Y under the same conditions (not shown). The 2255 cm^{-1} absorption was detected with Na−Y but the absorption was much smaller. The 2268 cm^{-1} absorption is also observed with Na−Y but is weaker than in BaNa−Y. This may be due to a weaker interaction between the intermediates absorbing at 2103 and 2171 cm^{-1} and Na^+ ions in Na−Y relative to the interaction with Ba^{2+} in BaNa−Y. This observation also suggests that the strength of the interaction could be affecting the kinetics of the surface reactions. As will be discussed below, most of these

surface species are likely ionic and thus are not expected to be stable in the gas phase.

The band at 2268 cm^{-1} gradually increases in intensity until ~14 s when its intensity starts to decrease. The molecule that is responsible for this absorption has the characteristic P, R band structure of a gas-phase molecule. Additional evidence consistent with this absorption being due to a gas-phase molecule is the fact that this absorption quickly disappears on evacuation of the cell. Gas-phase HNCO has been reported to absorb at 2268 cm^{-1},[41] and HNCO has been postulated as an intermediate in NO_x chemistry with hydrocarbons.[42,43] Thus, we assign the 2268 cm^{-1} absorption to HNCO.

A feature at 2255 cm^{-1} forms (see the 1 and 2 s spectra) and increases as a function of reaction time. Because of the increase in intensity of the gas-phase absorption at 2268 cm^{-1}, it is difficult to monitor the kinetics of the species absorbing at 2255 cm^{-1} over the entire time scale of the reaction. The bands at 2103 and 2171 cm^{-1} grow rapidly in intensity and reach a maximum after ~3 s. While the intermediate at 2171 cm^{-1} is barely seen after 6 s, the 2103 cm^{-1} species is clearly seen even after 14 s signaling that these absorptions belong to different intermediates. The 2103 cm^{-1} absorption disappears more slowly than the 2171 cm^{-1} absorption, but is negligible after 44 s.

The data presented thus far indicates that NO_2 oxidizes acetaldehyde to acetic acid via the pathway

$$CH_3(C{=}O)H + NO_2 \rightarrow CH_3(C{=}O)OH + NO \qquad (8)$$

NO_2 could also oxidize acetaldehyde to formaldehyde, possibly via the reaction

$$CH_3(C{=}O)H + 2NO_2 \rightarrow CH_2{=}O + CO + 2NO + H_2O \qquad (9)$$

However, though it will not be discussed in detail in this publication, there is also evidence that methanol is produced when acetaldehyde reacts with NO_2. Further, in separate experiments (not shown), we have observed that methanol reacting with NO_2 gives formaldehyde as a product. Thus, methanol could be a source of the observed formaldehyde.

Finally, in the presence of excess O_2, the NO can then be reconverted to NO_2. In this process, the oxidation state of the N atom thus oscillates between +2 and +4 until all acetaldehyde is oxidized. The acetic acid formed in eq 8 would be expected to rapidly convert to surface acetate.

D. Reactions of Acetic Acid + NO + O_2. Rapid scan FTIR spectra were taken to provide data on the fate of the surface acetate species on exposure to the NO + O_2 premix. Figure 5 shows spectral changes that take place for a BaNa−Y sample that was exposed to 0.4 Torr of acetic acid for 5 min at 473 K and subsequently evacuated at 473 K for 10 min (time $t = 0$ spectrum). After evacuation, the sample was exposed at 473 K to a gas-phase premix of 1.8 Torr of NO and 100 Torr of O_2 that was introduced into the cell with the rapid scan FTIR software running. The broad troughs in the spectrum at 1397, 1547, and 1664 cm^{-1} are due to loss in intensity of acetate absorptions which occur as a result of consumption by reaction with NO_2. It is possible that displacement of surface acetate by nitrate also contributes to this loss in intensity of the acetate absorptions. However, since as previously discussed, we have found that acetate displaces much of preadsorbed surface nitrate species on BaNa−Y, any displaced acetate would be expected to be more weakly bound than the majority of the surface acetate species. Though there is no evidence in the spectrum for growth of the band at 1789 cm^{-1} because of an absorption of gas-phase acetic acid, that absorption band is relatively weak and thus some gas-phase acetic acid could be present without being observable.

As previously discussed, the strong absorptions at 1341 (split into two bands) and 1443 cm^{-1} are due to surface-bound NO_3^-. The broad band at 1702 cm^{-1} is due to acetic acid that still resides on the surface, which is produced by the neutralization of a surface acetate species. Presumably, this is a more weakly bound species that interacts with BaNa−Y at different (or modified) sites than those that lead to surface acetate formation.

The gas-phase NO_2 absorption at 1616 cm^{-1} gradually decreases in intensity as a function of exposure time. Two products, N_2O and CO_2, which increase as a function of time, are seen at 2223 and 2348 cm^{-1}. The weak band at 1745 cm^{-1} is at the frequency of the strongest formaldehyde absorption and likely belongs to that molecule. As previously discussed, acetaldehyde also absorbs at 1745 cm^{-1}, but we cannot find a plausible reaction mechanism that produces acetaldehyde from the reaction of acetic acid with NO_2.

Three intermediates are observed at 2171, 2255, and 2268 cm^{-1}. All of these species were also observed in Figure 4. The gas-phase CO band that was present in Figure 4, at 2143 cm^{-1}, is not observed in Figure 5 on this time scale. The absence of the 2103 cm^{-1} absorption that was seen in Figure 4 is likely because its intensity is too small to be detected (compare the scale bar in Figure 5 with the one in Figure 4) and preadsorbed acetic acid could compete for the absorption sites that this species occupies. As previously discussed, experimental data indicate that the reaction of acetaldehyde with NO_2 leads to surface acetate. The data in section III. C and in this section indicate that surface acetate can form from either the reaction of NO_2 with acetaldehyde or directly from acetic acid. Once surface acetate is formed, there is a common set of reactions that occur with acetic acid as the starting material as with acetate formed from acetaldehyde. However, as discussed further in section IV. G the different CO_2/CO ratio with acetaldehyde and acetic acid as reactants is a clear indicator that there is at least one additional reaction channel that is *not common* to *both* acetaldehyde and acetic acid. We have performed experiments that have shown directly that CO *is not* oxidized to CO_2 over BaNa−Y under reaction conditions and thus the measured CO_2/CO ratio can be used as a direct indicator of the CO_2/CO ratio produced in this reaction system.

The fact that methanol is observed as a product when acetaldehyde is the reactant strongly suggests that there is an additional channel for the reaction of acetaldehyde with NO_2 relative to the reaction of acetic acid with NO_2. Consistent with this hypothesis, gas-phase nitromethane is observed when NO_2 reacts with acetaldehyde but not when the reactant is acetic acid.

To assist in the assignment of the intermediates alluded to above, ^{15}NO and both 1-^{13}C and 2-^{13}C-acetic acid were employed as reactants. Data from these experiments are shown in Figure 6 where spectrum a shows a spectrum obtained by exposing BaNa−Y to 1.4 Torr of acetaldehyde, 1.8 Torr of NO, and 100 Torr of O_2 at 473 K. The spectrum was obtained 6 s after the initial exposure. Spectrum b shows a spectrum obtained by exposing BaNa−Y to 1.4 Torr of acetaldehyde, 3 Torr of ^{15}NO, and 100 Torr of O_2 at 473 K. This spectrum was obtained 5 s after the initial exposure. Spectrum c was obtained under the same conditions as spectrum b but acetaldehyde was replaced by 0.4 Torr of acetic acid, and the spectrum was recorded 9 s after the initial exposure. Spectrum d was obtained under the same conditions as spectrum c except that acetic acid was

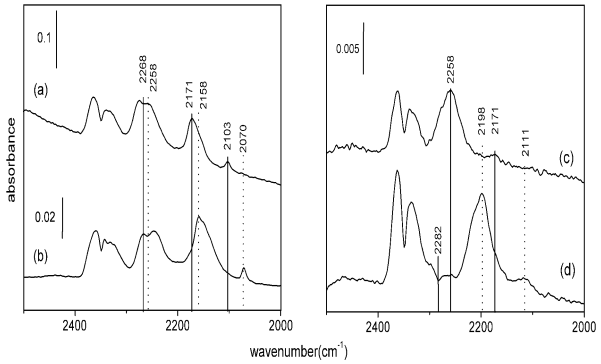

Figure 6. FTIR spectra of intermediate species observed on BaNa−Y at 473 K, (a) from acetaldehyde + NO + O_2, (b) from acetaldehyde + ^{15}NO + O_2, (c) from acetic acid + NO + O_2, and (d) from 2-^{13}C acetic acid + NO + O_2.

TABLE 1: Expected Isotopic Shift on Substituting ^{15}N for ^{14}N ($N \rightarrow {}^{15}N$)

	N	^{15}N	Δv	assignments	references
hydrogen cyanide, HCN	2090	2058	32	vCN	41
isocyanic acid, HNCO	2266	2258	8	v_{as}(NCO)	41
isocyanic acid dimer, $(HNCO)_2$	2259	2251	8	v_{as}(NCO)	41
formonitrile oxide, HCNO	2196	2152	44	v(CN)	95, 96
cyanide, CN^-	2112	2079	33	v(CN)	97
cyano, SiCN	2218	2188	30	v(CN)	98
isocyano, SiNC	2100	2064	36	v(NC)	98
isocyanato, SiNCO	2313	2303	10	v_{as}(NCO)	98
cyanate, KOCN or NaOCN	2170	2152	18	v(NC)	99
fulminate, HgONC	2202	2165	37	v(CN)	99

replaced by 2-^{13}C acetic acid and the spectrum was recorded 10 s after the initial exposure.

In spectrum a absorptions due to intermediates are seen at 2103, 2171, and 2268 cm^{-1}. The two species at 2171 and 2268 cm^{-1} show similar red shifts, Δ, when ^{14}N is replaced by ^{15}N, with $\Delta = 13$ and $\Delta = 10$ cm^{-1}, respectively (compare spectra a and b). On the other hand, the red shift of the species at 2103 cm^{-1} is $\Delta = 33$ cm^{-1}. In spectrum c two intermediate species are seen at 2171 and 2258 cm^{-1}. When acetic acid that is labeled with a ^{13}C at the methyl carbon ($^{13}CH_3C(O)OH$) is used as the reactant, both of the absorptions at 2258 and at 2171 cm^{-1} show the same red shift of $\Delta = 60$ cm^{-1} (compare spectra c and d). A weak gas-phase feature centered at 2282 cm^{-1} is due to $^{13}CO_2$.

The asymmetric stretching vibration of the N═C═O group has been reported to shift ∼8−10 cm^{-1} as a result of a change from ^{14}N to ^{15}N and ∼60 cm^{-1} as a result of ^{13}C labeling (see Table 1). As previously indicated, the position of the 2268 cm^{-1} absorption is in good agreement with literature values for gas-phase HNCO. From the data in ref 41, 2268 cm^{-1} is the midpoint between the P and R branch. The isotopic shifts are as expected for this compound. Thus, the 2268 cm^{-1} absorption is unambiguously assigned to gas-phase HNCO.

The 2258 cm^{-1} absorption is consistent with regard to position and isotope shift with an NCO group. This species is at lower frequency than gas-phase HNCO, and this absorption disappears on evacuation of the cell. This absorption's behavior is consistent with what would be expected for weakly adsorbed HNCO, but we cannot rule out another molecular species containing an NCO moiety.

The 2171 cm^{-1} band has a Δ of 60 cm^{-1} on ^{13}C substitution (spectrum c) and this absorption does not change in intensity when the cell is evacuated. This is consistent with a surface-bound NCO species, which could be NCO^-. In prior studies of HNCO adsorbed onto a metal oxide or metal surfaces, absorptions have been reported in the 2170−2200 cm^{-1} region. However, there has been disagreement about the assignment of the nature of this species.[44] On the basis of isotope shifts, it is unlikely that the 2171 cm^{-1} absorption seen in our work is due to fulminate (C═N−O^-), cyano (−C≡N^-), or isocyano (−N≡C^-), since the isotopic shifts (^{15}N) for these species are typically ∼37, ∼30, and ∼36 cm^{-1}, respectively (see Table 1). Similarly, it is unlikely that this absorption is due to an M^+---$^-$OCN ($M^+ = Na^+$ or K^+) species since such absorptions have been reported to shift ∼18 cm^{-1} in going from ^{14}N to ^{15}N (see Table 1). On the basis of the isotopic shifts of 10 cm^{-1} ($N \rightarrow {}^{15}N$) and 60 cm^{-1} ($C \rightarrow {}^{13}C$), the 2171 cm^{-1} absorption is best assigned to Ba^{2+}---N═C═O.

The peaks at 2268 and 2258 cm^{-1} (see spectra a and b) have a major contribution from both gas-phase (2268 cm^{-1}) and weakly adsorbed (2258 cm^{-1}) HNCO. The 2258 and 2198 cm^{-1} (which appears with 2-^{13}C acetic acid, see spectra c and d) absorptions are dominated by adsorbed HNCO and $HN^{13}CO$, respectively. The bands assigned to gas phase (with a band centered at 2268 cm^{-1}) and what we tentatively assign as weakly adsorbed HNCO as well as possibly to NCO^- (2171 cm^{-1}) all grow in more slowly with acetic acid as the reactant than with acetaldehyde (Figures 4 and 5)

The isotopic shift ($N \rightarrow {}^{15}N$) of the 2103 cm^{-1} absorption is 33 cm^{-1}. Both −CN and −NC have similar ^{15}N shifts of ∼30 and ∼36 cm^{-1}, respectively. The ^{15}N shift in CNO^- is 37 cm^{-1} and 44 cm^{-1} in HCNO. Such a surface species could desorb as HCNO, which is unstable in the gas phase, but could quickly isomerize to the more stable isocyanic acid. It is conceivable that CNO^- exists as an ionic species in a zeolite environment where it is associated with exchanged cations. There are similar isotopic shifts for covalently and ionically bonded CN (or NC), so all or any of the three species, M--$^-$NC, M--$^-$C≡N, and M--$^-$O−N═C ($M = Ba^{2+}$), could be responsible for or contribute to the band at 2103 cm^{-1} (see Table 1).

For a partial pressure of 0.4 Torr of acetic acid (Figure 5), the total amount of acetic acid consumed, as a result of reaction with NO_2, is only ∼15% of the initial amount adsorbed, even after a reaction time of 191 s. This indicates that the rate of consumption of surface acetate is slower than the corresponding rate of consumption of gas-phase acetaldehyde. The acetaldehyde band is completely gone after ∼5 min, while there is still acetic acid present even after 10 h. Indeed, for a gas mixture containing 1000 ppm NO_2, 50−100 ppm acetic acid, 9% O_2, 2% H_2O, and a GHSV of 30 000 h^{-1}, interacting with BaNa−Y at 473 K, only 15% of NO_2 was reduced to N_2 under experimental conditions (not shown). With the same NO_2 and H_2O concentrations, at the same temperature and GHSV, reduction of NO_2 to N_2 exceeded 90% with 50−100 ppm acetaldehyde (not shown, see ref 16 for experimental details). There are several possible explanations for these differences between the two reacting systems. If exchanged Ba^{2+} is involved in NO_x reduction, and there is a high concentration of surface acetate, there would only be limited adsorption sites for NO_x and the rate of reaction between NO_2 and surface acetate would be reduced if acetate blocked the channels or sites that NO_2 has to access for such a reaction to take place. This behavior is consistent with the observation that for low concentrations of acetic acid (little surface acetate), surface acetate reacts more rapidly.

With acetaldehyde as the starting material, results indicate that surface acetate does not build up on BaNa−Y for flowing reaction conditions since the reduction rate for NO_x with acetaldehyde did not change even after 10 h.[16] This is likely due to a smaller steady-state concentration of surface acetate

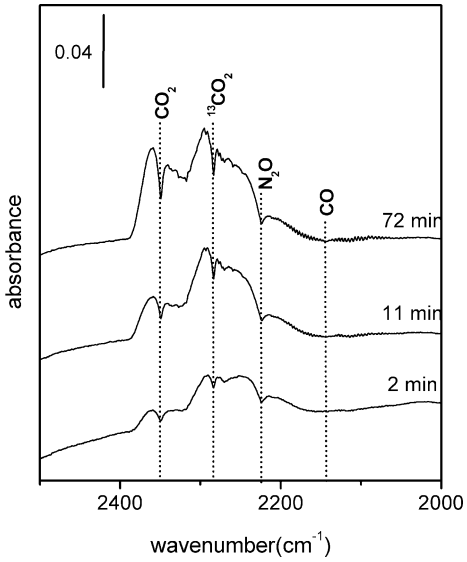

Figure 7. FTIR spectra of gaseous products obtained by exposing BaNa−Y to 1-^{13}C acetic acid + NO + O_2 at 473 K. The exposure time is indicated on each spectrum.

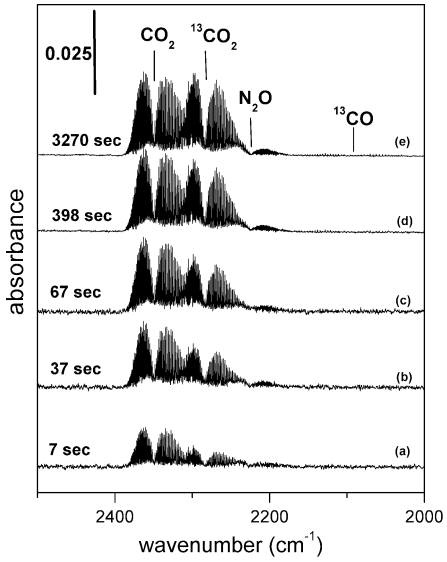

Figure 8. FTIR spectra of gaseous products obtained by exposing BaNa−Y to 2-^{13}C acetic acid + NO + O_2 at 473 K. The exposure time is indicated on each spectrum.

for these reaction conditions. It is evident from Figures 4 and 5 that part of the acetaldehyde is oxidized to surface acetate which is then oxidized further.

Figure 7 shows FTIR spectra obtained by exposing BaNa−Y to a premix of 3.6 Torr of NO and 100 Torr of O_2 at 473 K. Since at lower pressures of NO_2 the reaction with acetic acid is slow, the reaction rate was increased by doubling the amount of NO (3.6 Torr) relative to a typical premix (1.8 Torr of NO). Prior to exposure to this premix, BaNa−Y was preexposed to 0.4 Torr of 1-^{13}C acetic acid at 473 K.

Four absorptions are readily observable in the 2000−2500 cm^{-1} region at 2148, 2223, 2282, and 2348 cm^{-1}. These four absorptions are readily assignable to CO, N_2O, $^{13}CO_2$, and $^{12}CO_2$, respectively.[23] ^{13}CO would be expected at ∼2100 cm^{-1} since ^{13}CO shifts 48 cm^{-1} relative to ^{12}CO.[45] With the 1-^{13}C isotopomer of acetic acid, ^{13}CO is not detected indicating that no detectable CO comes from the methyl carbon of acetic acid. This sequence is summarized in eq 10.

$$\mathrm{CH_3(^{13}C{=}O)OH + NO_2 \rightarrow\ ^{13}CO_2 + \text{C-containing intermediates} \rightarrow\ CO_2 + CO + \text{other products}} \quad (10)$$

Unlike in Figure 5, the intermediate at 2255 cm^{-1} is not seen in the spectrum taken 2 min after exposure to the premix. The difference in concentration of this intermediate is a result of the difference in NO_2 pressure. At a higher pressure of NO_2, the lifetimes of all the intermediates which were previously discussed are significantly reduced and thus do not build up to as high a steady-state concentration, and the maximum steady-state concentration is expected to occur earlier in the reaction. Another factor favoring an earlier maximum in the concentration of intermediates is that the rate of reaction of acetic acid with NO_2 increases with increasing NO_2 concentration.

The formation of $^{12}CO_2$, $^{13}CO_2$, and CO was investigated in more detail using the other isotopomer, 2-^{13}C acetic acid. Figure 8 shows gas-phase FTIR spectra obtained at 0.5 cm^{-1} resolution by exposing BaNa−Y to a premix of 0.1 Torr of 2-^{13}C acetic acid, 3.6 Torr of NO, and 100 Torr of O_2 at 473 K. Spectra a−c were obtained by averaging four scans to obtain better time resolution in the early stages of the reaction. The data for spectra d and e were obtained by averaging 40 scans to obtain better signal-to-noise levels for longer reaction times. At modest pressures of 2-^{13}C acetic acid (0.1 Torr), there is more $^{12}CO_2$ relative to $^{13}CO_2$ at early reaction times. However, the final concentrations of $^{12}CO_2$ and $^{13}CO_2$ are, as expected, approximately equal. The difference in the formation rates of the two different isotopically labeled CO_2 molecules can be explained as follows. The $^{13}CO_2$ must come from the methyl carbon and its incorporation into CO_2 clearly must involve several reaction steps. Whereas the $^{12}CO_2$, which comes from the carboxylic acid group, could be directly eliminated or displaced by NO_2.

Consistent with this explanation is the fact that it is only in the last two spectra that ^{13}CO has a large enough intensity to be observable above the noise level of the spectrometer. If any ^{12}CO forms, it is present at a lower concentration than ^{13}CO. Interestingly, the rates of formation of $^{12}CO_2$ relative to $^{13}CO_2$ change with the concentration of acetic acid: At a higher partial pressure of acetic acid (0.4Torr), the rate of formation of $^{13}CO_2$ relative to $^{12}CO_2$ is much less than at 0.1 Torr partial pressure (not shown). This is again consistent with there being separate kinetic channels for the formation of $^{12}CO_2$ and $^{13}CO_2$.

E. Identification of CH_3NO_2 and Its Reactions. Figure 9 shows gas-phase FTIR spectra obtained from a sample of BaNa−Y that had been exposed to 4 Torr of acetaldehyde at 373 K and then had a premix of 2 Torr of NO and 100 Torr of O_2 added to the cell for an exposure time of 72 min at 373 K. To increase the amount of gas-phase products, ∼50 mg of BaNa−Y was used in this experiment.

Spectrum a was obtained by subtracting the gas-phase absorptions of NO_2 from the resulting spectrum. Two new gas-phase products are seen at 1583 and 3311 cm^{-1}. The 3311 cm^{-1} feature is readily assigned to gas-phase HCN on the basis of its position and rotational spacing. Its intensity slowly decreases with time. The genesis of this HCN and the chemistry of its consumption are under study.

The inset in Figure 9 shows an expansion of the region between 1300 and 1650 cm^{-1}. The top spectrum in the box is a gas-phase spectrum of an authentic sample of CH_3NO_2. The shape and position of the band centered at 1583 cm^{-1} in spectrum a are in excellent agreement with that of authentic CH_3NO_2. Accordingly, this band is assigned to gas-phase

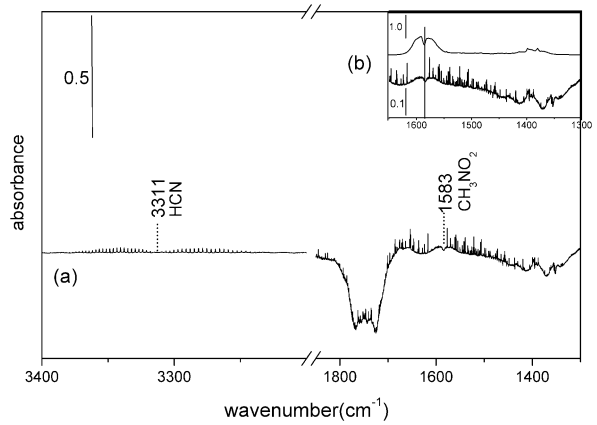

Figure 9. FTIR spectra of gaseous products produced from the reaction of acetaldehyde + NO + O_2 reaction on BaNa−Y at 373 K. The region between 1600 and 1300 cm^{-1} is expanded in the insert. The top spectrum in the inset is the FTIR spectrum of gas-phase CH_3NO_2.

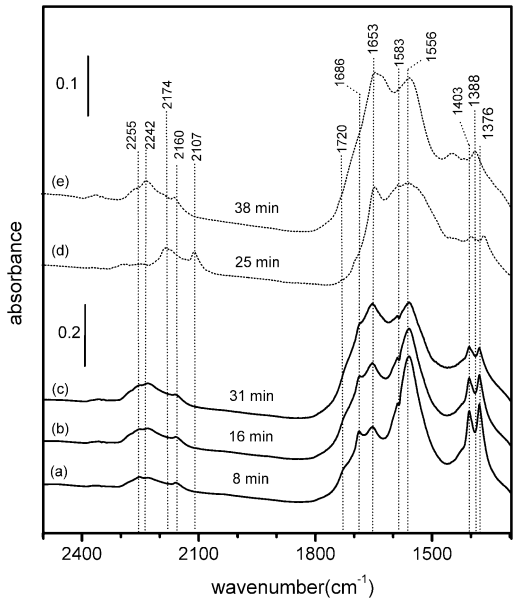

Figure 10. FTIR spectra obtained upon exposing dehydrated BaNa−Y to (a)−(c) 1.2 Torr of CH_3NO_2 (solid line), (d) $^{13}CH_3NO_2$, and (e) CD_3NO_2. Exposure times at 473 K are indicated on each spectrum.

CH_3NO_2. Adsorbed nitromethane (NM) was not detected. Though as discussed below there is evidence for gas-phase NM at the typical reaction temperature of 473 K with acetaldehyde as a reactant, the concentration of NM at 473 K is low and direct observation and assignment of NM required a lower sample temperature of 373 K, where the concentration of NM was higher and the absorption of NM more distinct. The "negative" features between 1300 and 1450 cm^{-1} and centered at 1745 cm^{-1} are due to consumption of gas-phase acetaldehyde as a result of its reaction with NO_2. Features due to gas-phase H_2O are seen between 1350 and 1850 cm^{-1}. The data in Figure 9 indicate that both NM and HCN are produced in the reaction of acetaldehyde + NO + O_2 on BaNa−Y.

Since nitromethane is produced in the reaction of acetaldehyde with NO_2, the chemistry resulting from the interaction of NM with BaNa−Y was investigated by starting with authentic samples of CH_3NO_2, $^{13}CH_3NO_2$, or CD_3NO_2, which were introduced into the cell containing BaNa−Y at 1.2 Torr pressure at 473 K (see Figure 10). The spectra show the spectral changes that take place for CH_3NO_2 (a−c), $^{13}CH_3NO_2$ (dotted spectrum d), and CD_3NO_2 (dotted spectrum e), as a function of exposure time. In the solid spectra, an absorption due to adsorbed NM is seen at 1556 cm^{-1}. An absorption in this region is consistently reported for adsorbed NM though the precise frequency varies as a function of the material it is adsorbed on.[46] Absorptions due to gas-phase NM can be seen centered at 1583 cm^{-1} (partially obscured by adsorbed NM) and at 1376 and 1403 cm^{-1}.[46] The bands of NM gradually decrease in intensity as a function of exposure time and new bands at 1653 (strong), 2160, and 2242 cm^{-1} (broad, with several features) emerge and increase in intensity as a function of time. Two bands at 1686 and 1720 cm^{-1} (shoulder) are absent at very early time (not shown) but grow in with time and thus cannot be due to NM absorptions. These two bands are seen in spectrum e but because of the ^{13}C isotopic shift of the C═O group these bands are not seen in spectrum d. The 1720 cm^{-1} band is shifted to 1686 cm^{-1} in spectrum d and, on the basis of the typical isotopic shift (C→^{13}C) of a C═O vibration in carbonyl compounds of ∼40 cm^{-1},[47] the 1688 cm^{-1} absorption is expected to shift to ∼1648 cm^{-1}. At ∼1648 cm^{-1}, the absorption would be masked by the strong absorption band centered at 1653 cm^{-1} that is due to adsorbed NM.

After exposure of BaNa−Y to NM, the NO_2 vibration of adsorbed NM at 1556 cm^{-1} decreases in amplitude and a new absorption at 1653 cm^{-1} appears and grows. Thus, there are two intermediates that form from NM. One has a C═O stretch at 1720 cm^{-1}, and the other has a vibration at 1653 cm^{-1} that does not shift significantly on ^{13}C or D substitution (see spectra d and e). Therefore, the absorption of this second intermediate at 1653 cm^{-1} does not correspond to a C═O or H vibration. Thus, we conclude that the 1653 cm^{-1} vibrational mode is a normal mode that involves primarily motion of N and O atoms.

The literature provides some insights into what species could give the aforementioned behavior. Since the surface is exposed to only nitromethane, it is logical to first look at whether one of the many isomers of nitromethane could correspond to these intermediates. Two isomerization pathways of interest to this work involve the formation of methyl nitrite and the formation of formohydroxamic acid, which has been reported to be a potential precursor to HNCO.[48,49] It has also been reported that methyl nitrite can form directly via the unimolecular rearrangement of nitromethane.[48,50] Methyl nitrite has an ONO group vibration in the expected frequency region, and there is a minimal shift in the frequency of the ONO vibration on ^{13}C or D substitution. The ONO vibration in the three isotopomers of trans-methyl nitrite, $^{12}CH_3NO_2$, $^{13}CH_3NO_2$, and CD_3NO_2, are all reported at ∼1677 cm^{-1} in the gas phase.[51] We cannot identify any other plausible molecules that could result from NM that contain functional groups containing only N and O atoms with vibrational frequencies in the necessary spectral range. Though it is conceivable that the absorption is due to an oligomer of NM, it would have to be a very unusual species which contained an ONO vibration. Hence, the most plausible candidate for the 1653 cm^{-1} absorption is simply methyl nitrite.

Adsorbed methyl nitrite had been reported on a Ag surface and it had been stabilized by the interaction of the lone pair electrons of the internal oxygen with a Ag surface.[52] By analogy, the lone pair electrons of methyl nitrite could be stabilized by interaction with Ba^{2+} ions.

Isomerization of NM to methyl nitrite has a barrier of 64.6 [48] and 69 kcal/mol.[50] Because of these relatively high gas-phase barriers, this isomerization process would be expected to be insignificant on the time scale of the experiments in this study. Thus, the barrier for isomerization to methyl nitrite must be lower for adsorbed NM.

SCHEME 1

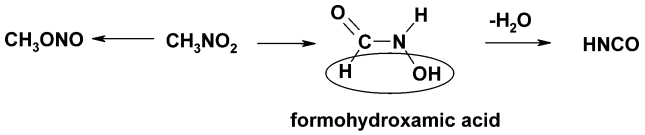

TABLE 2: Expected Isotopic Shift on Substituting ^{13}C for ^{12}C ($C \rightarrow {}^{13}C$)

	C	^{13}C	isotopic shift ($\Delta\nu$)	assignments	references
HNCO	2266	2206	60	ν_{as}(NCO)	95
$(HNCO)_2$	2259	2200	59	ν_{as}(NCO)	95
SiNCO	2313	2252	60	ν_{as}(NCO)	98

We now turn our attention to the species that could be responsible for the absorption at 1720 cm^{-1} which shifts to 1688 cm^{-1} on ^{13}C substitution. 1720 cm^{-1} is too high a frequency for the NO stretch (1549 cm^{-1}) in nitrosomethane[53] and also for the C−N stretch of any of the NM isomers with a C═N moiety. The isotope shift is characteristic of what would be expected for a carbonyl moiety.[47] Thus, the most likely candidate is formohydroxamic acid (HC(O)NH(OH)) which is the only isomer on the calculated potential energy surface for NM that has a carbonyl moiety. The trans isomer of formohydroxamic acid has a gas-phase absorption at 1731 cm^{-1} while the cis isomer absorbs as 1683 cm^{-1}.[54] Formohydroxamic acid has been reported to form in the gas phase via the rearrangement of aci-nitromethane, which in turn can form via a direct unimolecular rearrangement of NM. Formohydroxamic acid can then lose water to form HNCO. This pathway to HNCO from NM has been proposed in several studies of deNO_x reactions.[42,43,49] These processes are shown in Scheme 1.

Given these assignments, the kinetics observed in Figure 10, in which methyl nitrite continues to grow while the growth of formohydroxamic acid is terminated and even decreases, implies that the reaction of NM to form methyl nitrite is not readily reversible while, as expected, formohydroxamic acid dehydrates and forms HNCO. A different pattern of absorptions is seen in the 2100−2400 cm^{-1} region when starting with nitromethane versus those generated by the reaction of acetic acid or acetaldehyde with NO_2. With NM as the starting reactant, there are two bands which are observed at 2160 and 2242 cm^{-1} (broad) that are *not* observed under experimental conditions when acetic acid or acetaldehyde reacts with NO_2. The ^{13}C isotopic shift for the species at 2160 and 2242 cm^{-1} are 53 and ∼68 cm^{-1}, respectively (compare spectra c and d of Figure 10). Isotopic shifts of this magnitude for absorptions in the relevant spectral region have been reported for molecules containing N═C═O or N═C═N groups (see Table 2). The 2255 cm^{-1} absorption is likely due to weakly adsorbed HNCO that is also seen in Figures 4 and 5. Weakly adsorbed HNCO absorbs at 2255 cm^{-1} on both BaNa−Y and NaY. Thus, some contribution to the 2255 cm^{-1} absorption observed in Figures 4 and 5 from interaction with Na^+ cannot be ruled out. However, on the basis of the intensity of the 2255 cm^{-1} adsorptions on BaNa−Y and NaY, we would expect a contribution from an interaction of HNCO with Na^+ to be minor.

The bands at 2242 and 2160 cm^{-1} in Figure 10 are shifted to lower frequency than the corresponding bands in Figure 4. Thus, a plausible candidate for these absorptions is dimerized isocyanic acid $(HNCO)_2$. The formation of such a dimer will be favored by the higher concentration of NM in the zeolite cavities. The concentration of NM in the zeolite cavities would be expected to be higher in the absence of NO_2 and when NM is introduced as a neat gas-phase species.

The bands at 2242 (broad), 2160, and 2255 cm^{-1} may be due to cyanamide (carbodiimide). The strongest bands of carbodiimide in solution are observed at 2245 and 2224 cm^{-1} [55] and at 2248 and 2225 cm^{-1} in solid cyanamide. A $C \rightarrow {}^{13}C$ shift of a N═C═N group is typically ∼61 cm^{-1}.[56] When an authentic sample of cyanamide was introduced into Ba−Y at 473 K, bands were observed at 2242 and ∼2157 cm^{-1} (not shown). However, the exact frequency of the lower energy band depended on experimental conditions.

The species that absorb at 2160, 2242, and 2255 cm^{-1}, which are formed by introducing NM into BaNa−Y at 473 K, do not rapidly decompose at 473 K and are not effected by addition of NO or O_2 individually. However, adding water (not shown) increases the decomposition rate of these species, but this rate is still much slower than the rate of reaction of the aforementioned species with NO_2 even though the partial pressure of water that was introduced into the cell was higher than that of NO_2. The authentic sample of cyanamide also reacted rapidly when NO_2 was added to the cell.

The polymerization of HNCO has been reported to lead to a mixture of cyanuric acid, cyamelide, and other oligomers with the formula $(HNCO)_n$.[57] Of all the polymerization pathways for HNCO in the gas phase, it has been reported that formation of an isomer of cyanuric acid ($C_3N_3O_3H_3$) is thermodynamically the most favorable. However, association of three HNCO molecules could be subject to a kinetic constraint under our experimental conditions. Thus, the formation of cyanamide (H_2N═C≡N), which requires two HNCO molecules, could be kinetically more facile, since it could form by dimerization and decarboxylation when HNCO accumulates in the channels of BaNa−Y.

$$2HNCO \rightarrow H_2N{-}C{\equiv}N + CO_2 \qquad (11)$$

Cyanamide exists as a tautomer with carbodiimide (HN═C═NH).[58] The formation of cyanamide from HNCO has been studied both theoretically and experimentally[57,59,60] and its reaction with water has also been studied by theory and experiment.[58]

An ionic form of carbodiimide is also possible. The anion and dianion of carbodiimide are known and could be stabilized in a zeolite environment. The carbodiimide $(N{\equiv}C{-}NH)^-$ anion and carbodiimide dianion $(N{\equiv}C{-}N)^{2-}$ can form metal salts.[61,62] In crystals of cyanamide metal salts, the range of frequencies for the NCN group is 1930−2114 cm^{-1}.[60] These frequencies are considerably removed from those cited above. However, a blue shift of the −C≡N vibration on BaNa−Y is possible if there is more triple bond character to the C≡N group when intereacting with Ba^{2+} ions than when the group is incorporated in a salt lattice.

Carbodiimide anion could form via the following process from cyanamide along with a proton that presumably would associate with the framework oxygens.

$$Ba^{2+}\text{---}HN{=}C{=}NH \rightarrow Ba^{2+}\text{---}(N{=}C{=}NH)^- + H^+ \qquad (12)$$

Cant et al. have proposed that cyclic compounds, cyanuric acid, ammelide, ammeline, and melamine, are formed by oligomerization of HNCO upon introducing CH_3NO_2 into Co−ZSM-5.[43] The carbodiimide species can also be a precursor for the cyclic compound, ameline[58a] which has been reported to form by reaction with NH_3 under appropriate catalytic conditions.[43] These cyclic compounds have not been observed on BaNa−Y for our reaction conditions. This is probably because of the lower reaction temperature relative to the study in ref 63.

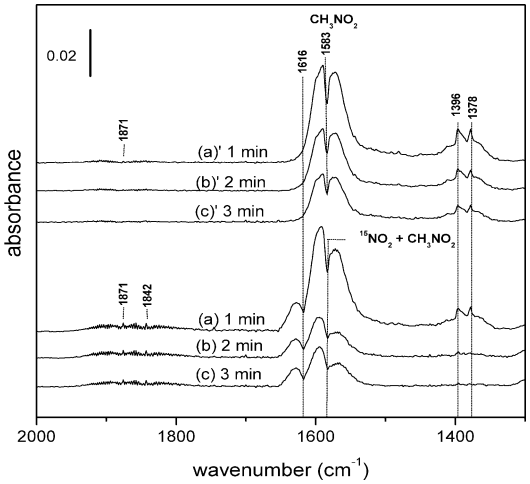

Figure 11. Gas-phase FTIR spectra obtained by exposing BaNa−Y at 473 K to (a)−(c) a premixed gas mixture of nitromethane + ^{15}NO + O_2 and to (a)′−(c)′ a premixed gas mixture of nitromethane + O_2. The exposure time is indicated on each spectrum.

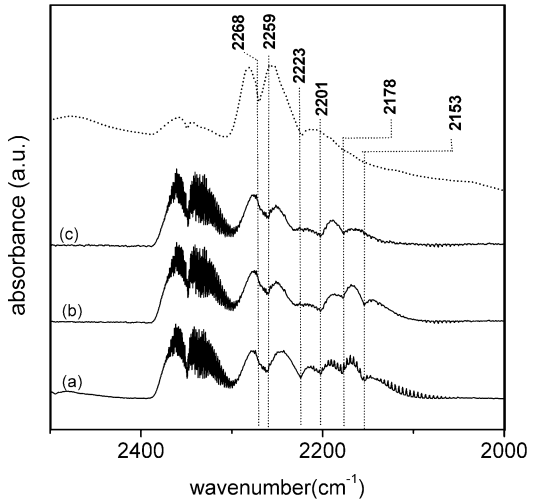

Figure 12. FTIR spectra of gaseous products produced from CH_3NO_2 + NO + O_2 (dotted spectrum) and CH_3NO_2 + ^{15}NO + O_2 (spectrum a) reaction on BaNa−Y at 373 K. (b) The gas-phase spectra of pure N_2O and CO are subtracted from spectrum a and c; the spectrum of pure $^{15}N^{15}NO$ is subtracted from spectrum b.

The thermal reaction of NM in the absence of other reactants in BaNa−Y at 473 K is slow as judged from the fact that the intensity of the gas-phase absorption of CO_2, a product of this reaction, is relatively small even after 31 min at 473 K. The rate of appearance of CO_2 increased somewhat when water was added but was not affected by adding either NO or O_2 separately (not shown here). If NM is introduced into BaNa−Y simultaneously with a NO and O_2 premix, NM reacts rapidly with NO_2 and the intermediates assigned as CH_3ONO and $(HNCO)_2$ and the N═C═N absorption did not build up on BaNa−Y. This implies that NO_2 plays a key role in the thermal reactions of CH_3NO_2. In fact, the data discussed below and in section IV. E indicate that in the presence of NO_2, there are different and more efficient pathways for the formation of HNCO.

Gas-phase spectra shown in traces a−c in Figure 11 were obtained by exposing BaNa−Y to a premix of 1 Torr of nitromethane + 1 Torr of NO + 100 Torr of O_2 at 473 K. The gas-phase spectra in traces a′−c′ are obtained by exposing BaNa−Y to a premix of 1 Torr of NM + 100 Torr O_2 at 473 K. The bands at 1378 and 1396 cm^{-1} in spectrum a and in spectra a′−c′ are due to NM. The band centered at 1583 cm^{-1} in spectrum a is due to $^{15}NO_2$ and NM and in spectra a′−c′ only to NM. The band centered at 1616 cm^{-1} in spectra a−c is due to NO_2. The 1842 cm^{-1} absorption in spectra a−c is due to ^{15}NO and the band at 1871 cm^{-1} in spectra a−c and a′−c′ is due to NO.

In the presence of NO_2, the rate of reaction of NM is much more rapid than in the absence of NO_2 as evidenced by the much more rapid disappearance of the NM absorptions at 1396 and 1378 cm^{-1} in spectra a−c relative to a′−c′ in Figure 11. Equally important is the appearance of a NO_2 absorption in the lower traces when the reaction mixture contained $^{15}NO_2$ + NM. $^{14}NO_2$ appears rapidly and is then consumed as a result of its reaction with NM and likely with reaction intermediates. We have also demonstrated that even though NM does exchange its NO_2 moiety with labeled NO_2 in the gas phase, this reaction is much slower than the reaction shown in Figure 11. Thus, the generation of $^{14}NO_2$ on the time scale shown in Figure 11 must be due to a surface process, which will be discussed in more detail in Section IV. E.

Figure 12 shows gas-phase spectra obtained after exposure of BaNa−Y at 373 K to 7 Torr of NM and 1 Torr NO (upper trace) or to 2.3 Torr NM, 1 Torr of ^{15}NO, and 100 Torr of oxygen. The spectra were taken at relatively low temperature (373 K) since the rate of reaction of the HNCO (or $H^{15}NCO$) that is produced is too fast to be monitored at 473 K in the presence of NO_2. To increase the amount of the HNCO and the N_2O gas-phase products, 50 mg of BaNa−Y was used for this experiment. The bands centered at 2223 and 2268 cm^{-1} are due to N_2O and HNCO, respectively (see dotted spectrum). There are multiple absorption bands between 2050 and 2223 cm^{-1} which are not observed in the dotted spectrum. The well-resolved gas-phase feature centered at 2151 cm^{-1} is due to CO. To identify the species that produce the other absorptions, the gas-phase spectra of $^{14}N^{14}NO$ (centered at 2223 cm^{-1}) and CO were subtracted from spectrum a with the resulting spectrum shown in spectrum b. It is clear that this spectrum contains a contribution from $^{15}N^{15}NO$ centered at 2153 cm^{-1}, and therefore the spectrum of $^{15}N^{15}NO$ was subtracted from spectrum b with the resulting spectrum shown in trace c. After these subtractions, it is clear there are two additional species with absorptions centered at 2178 and 2201 cm^{-1} which contribute to the spectrum. These frequencies match the literature frequencies for $^{14}N^{15}NO$ and $^{15}N^{14}NO$.[64] Thus, the data in Figure 12 demonstrates that the four isotopomers of N_2O are produced from the reaction of NM + ^{15}NO + O_2.

Additionally, as expected, both HNCO and $H^{15}NCO$ are produced in this reaction. HNCO has an absorption band that is centered at 2268 cm^{-1} (upper spectrum in Figure 12 and see Figure 4). $H^{15}NCO$ is expected to have an absorption that is shifted by ~9 cm^{-1} relative to HNCO (see Table 1) and thus is expected to be centered at 2259 cm^{-1}. The shape of the absorption band in this region in spectra a−c makes it clear that both HNCO and $H^{15}NCO$ contribute to this band. The proposed mechanism for production of these species will be discussed in the following section.

The reaction of HNCO with NO_x has drawn considerable interest because of its relevance to the RAPRENO$_x$ (rapid reduction of NO_x) process.[65,66] Incomplete hydrolysis of HNCO has been evident at low temperature and high space velocity and this has been a major problem in the use of urea as an NH_3 source on oxide catalysts. Lin et al. studied the gas-phase thermal reaction of HNCO with NO_2 from 623 to 773 K using FTIR.

Isocyanic acid is easily hydrolyzed on various oxides such as silica, alumina, and titania and also on typical SCR catalysts.

Poignant had identified it as the precursor for ammonia on Cu/ZSM-5 catalysts.[67] On metal catalysts such as Pt/Al_2O_3 and Pt/TiO_2 some authors report that isocyanate causes deactivation of the metal sites.[44] Cant et al. have proposed that a Co−ZSM-5 catalyst was deactivated by formation of s-triazine and on that surface NCO formed when CH_3NO_2 interacted with the catalyst at 553 K.[43] Upon adding NO_2, the s-triazine compounds that formed rapidly decomposed to N_2 and CO_2, while surface NCO was not removed. These authors also report that surface isocyanate was produced when a Cu-MFI catalyst was deactivated by the s-triazine compounds. Hydrolysis of the isocyanate species was far from complete when water was added to a deactivated catalyst.[68] On the other hand, the Rh−NCO complex, observed on Rh foil and a Rh monocrystalline surface, is very unstable.[44]

The hydrolysis of HNCO has been investigated on various oxide catalysts, including TiO_2, V_2O_5/TiO_2, and V_2O_5–WO_3/TiO_2 and it has been investigated in solution.[69b] The conversion of HNCO is high even at high space velocities (10^6 h^{-1}) and low temperatures (423 K). The highest rate for the hydrolysis of HNCO was on pure TiO_2 powder. For the present experimental conditions, the rapid hydrolysis of HNCO on BaNa−Y in the presence of NO_2 may be due to a lowering of the activation energy for the reaction under acidic conditions.

There is evidence in the literature that hydrolysis of isocyanates is accelerated in acidic solution.[69a] The activation energy for the hydrolysis of HNCO is 14.5 kcal/mol in hydrochloric or nitric acid solution. When water is present, upon introducing NO_2 into BaNa−Y, the zeolite environment becomes more acidic. The hydrolysis process could follow a pathway such as that shown below in eq 13.

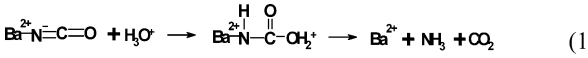

(13)

F. The Reaction of Nitric Acid and Ammonia. Two drops of diluted HNO_3 solution (40%) were dropped onto 15 mg of a dried BaNa−Y sample which had been painted on the tungsten grid at 358 K. After this treatment, the sample was placed in the IR-cell and evacuated for 10 min at 298 K. The sample was then exposed to 27 Torr of NH_3. A detectable amount of N_2O was formed at ~433 K and more N_2O was produced by increasing the temperature to 473 K.

IV. Discussion

A. Reaction Mechanisms. As always in heterogeneous catalysis, the most reactive surface intermediates are expected to have an extremely low steady-state concentration at the reaction temperature, which makes their spectroscopic identification under those conditions difficult if not impossible. For zeolite-based catalysts, there exists abundant nonspectroscopic (mainly TPD and isotopic labeling) evidence that the low activation energy path for NO_x reduction to N_2 makes use of ammonium nitrite as the crucial intermediate.[12] It decomposes at a temperature below 373 K:

$$NH_4NO_2 \rightarrow N_2 + 2H_2O \qquad (3)$$

Ammonium nitrite is assumed to form from ammonia and nitrous acid, HONO.

The formation of HONO is easily understood, considering the equilibria

$$NO + NO_2 \rightarrow N_2O_3 \qquad (1)$$

and

$$N_2O_3 + H_2O \rightarrow 2HONO \qquad (2)$$

The mechanism for N_2 production via ammonium nitrite is operative on a variety of catalysts, as evidenced by the fact that the NO_x reduction rate is significantly higher with a 1:1 ratio of NO and NO_2 than with either pure NO_2 or NO.[70] In further support of this mechanism, the N_2O_3 and HONO intermediates have been identified by IR at low temperature on an Fe/MFI catalyst.[3,12]

The nontrivial part of this reaction mechanism is the formation of NH_3 from NO_x. In this study, ammonia is formed by reducing NO_2 with acetaldehyde over BaNa−Y. It is this reaction that the dicussion will focus on. The present data, mostly obtained at 473 K, provide a road map for the critical reactive steps. Hopefully, it will spur further detailed studies of this system and related systems and will help to frame attempts to identify other systems in which deNO_x reactions may be efficient. The steps involved in the reaction mechanism will be discussed in turn. However, the delineation of the elementary reactions involved in deNO_x chemistry presents a special mechanistic challenge: Because of the multiple equilibria in which NO_x species are involved, it may not always be possible to uniquely identify the major NO_x reactant in a given reaction.

B. Nitrate Formation. When BaNa−Y is exposed to NO_2, surface nitrates form. There are at least four reactions that could contribute to the formation of surface nitrates observed in this study.

$$NO^+ + NO_2 + H_2O \rightarrow 2H^+ + NO_3^- + NO \qquad (5)$$

$$3NO_2 + H_2O \rightarrow 2NO_3^- + 2H^+ + NO \qquad (6)$$

$$2NO_2 \rightarrow N_2O_4\ NO^+ + NO_3^- \qquad (4)$$

$$OH + NO_2 \rightarrow -NO_3^- + H^+ \qquad (7)$$

Two of these (5 and 6) involve water as a reactant while two (4 and 7) can occur in the absence of water.

As indicated in Section III. A, there are two types of surface nitrates; one is depleted on evacuation of the cell and the other remains on the surface even after evacuation. These nitrates exhibit different reactive behavior. The rate of reaction for the nitrate species which persists after evacuation (see spectrum b in Figure 2), with either acetaldehyde or acetic acid in the presence of O_2, at 473 K, is negligible. However, as discussed in Section III. A, weakly adsorbed NO_3^-, which is present prior to evacuation, could interact with other surface species or could serve as a source of NO_2. NO_2 can be also produced by desorption of the adsorbed NO_3^- via the back reaction in eq 4. That NO_2 can serve as a reactant for other species present in the system.

C. Reactions of Acetaldehyde. The chemistry of acetaldehyde is markedly different when BaNa−Y is exposed to only acetaldehyde versus when it is either preexposed to NO_2 or when it is exposed to a mixture of NO_2 and acetaldehyde. When BaNa−Y is exposed to acetaldehyde, there is facile formation of crotonaldehyde via an aldol condensation reaction.

Aldol condensation reactions are catalyzed by either acid or basic sites.[71] In this system, the reaction is expected to be accelerated by Lewis acid sites, such as Ba^{2+} ions, since adsorption increases the electrophilicity of the carbonyl carbon of acetaldehyde. Thus, the formation of crotonaldehyde should

SCHEME 2

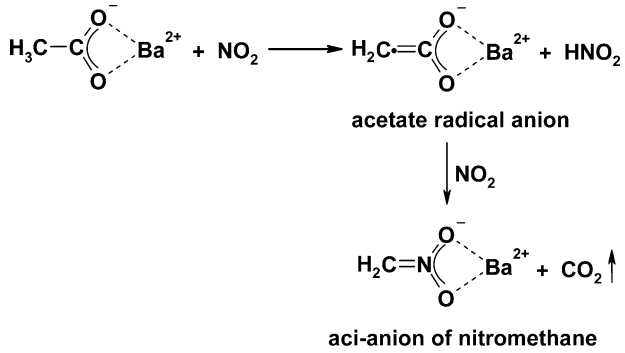

be inhibited if Ba^{2+} ions are previously exposed to a reactant that leads to the formation of surface nitrates and acetates which compete for these acidic sites. In addition, other reactants can provide a pathway for acetaldehyde consumption that competes with the aldol condensation reaction. On the basis of this reasoning, the actual amount of crotonaldehyde that forms in the presence of acetaldehyde plus the NO + O_2 premix would be expected to be significantly reduced. Indeed, we *have not* observed crotonaldehyde under reaction conditions where reduction of NO_2 is efficient (vida supra).

When BaNa−Y is exposed to a mixture of acetaldehyde and NO and O_2, acetaldehyde reacts with NO_2, which has formed in the premix, in preference to undergoing an aldol condensation reaction to form crotonaldehyde. The reaction that occurs leads to the formation of surface acetate species. Surface acetate can be produced either via reaction of NO_2 with acetaldehyde or as a result of adsorption of acetic acid. A crucial observation is that nitromethane is observed in the gas phase when acetaldehyde reacts with NO_2 at 373 K. There is also evidence for nitromethane formation at 473 K in the presence of acetaldehyde and NO_2.

D. Acetate Formation. As alluded to above, when the BaNa−Y sample is exposed to acetic acid, surface acetate is observed (see Figure 3 and Section III. B). Surface acetate suppresses surface nitrate formation. While surface nitrate is mostly removed by evacuation at 473 K, surface acetate is minimally changed as a result of evacuation, leading to the conclusion that surface acetate is a more strongly bound species than at least a significant fraction of the surface nitrate. As previously discussed, there are two types of surface nitrate species—one being more strongly bound than the other. There is evidence that the weakly adsorbed surface nitrate species can be displaced by surface acetate, where the displaced nitrate may undergo the reaction

$$2H^+ + 2NO_3^- \rightarrow NO_2 + NO + O_2 + H_2O \qquad (14)$$

The more strongly bound surface nitrate species is not readily displaced by acetate.

As previously discussed, both nitrate and acetate ions can form on BaNa−Y under experimental conditions. One plausible interpretation of the data in this study is that, as shown in Scheme 2, acetate ions ($CH_3CO_2^-$) are attacked by NO_2 to give the aci-anion of NM ($CH_2NO_2^-$), which could be stabilized by Ba^{2+} ions. Though we are not yet in a position to definitively delineate the microscopic mechanism for this transformation, one plausible pathway is shown in Scheme 2. In this scheme, acetate radical anions are produced as a product of the first step and they can subsequently couple with NO_2 to give the aci-anion of NM ($CH_2NO_2^-$).

Acetate anion radicals have been produced in a variety of chemical environments. The reaction between F_2 and enolate anions of acetic acid[72] and the reaction of OH with acetate ions have been reported to yield acetate anion radicals.[73] Wenthold et al. observed that acetate radical anions undergo gas-phase reactions with NO, SO_2, and NO_2 by CH_2^- transfer, forming CH_2NO^-, $CH_2SO_2^-$, and $CH_2NO_2^-$, respectively.[72]

E. The Formation and Reactions of Nitromethane. As indicated above, the aci-anion of NM could form directly from the acetate radical anion. The aci-anion of NM could then protonate and produce NM. There would then be an equilibrium between the aci-anion of NM and NM.

NM has been produced by reaction of partially oxygenated hydrocarbons, namely, ethanol, acetic acid, and acetaldehyde with HNO_3 (or NO_2) in the gas phase at high pressures and temperatures.[74,75] When neat NM is adsorbed onto BaNa−Y at 473 K, molecules containing a C═O group, most likely formohydroxamic acid, which can be produced by isomerization of aci-NM,[48,49] are detected. However, the aci-anion of NM itself is not detected on BaNa−Y.

Lack of direct observation of the aci-anion of NM on BaNa−Y implies that its steady-state concentration is low. This can be explained as follows: NM is moderately acidic (pK_a = 10.0) and the formation of the aci-anion of NM is enhanced by a strong base. As alluded to above, the aci-anion of NM has been observed in strong alkali solution (0.5 M NaOH solution).[76] The basicity of the framework oxygens of BaNa−Y is less than for Na−Y and Na−Y is less basic than Na−X and Cs−X. The aci-anion of NM has been observed on Na−X[77] and Cs−X,[78] but not in the more acidic zeolite, HZSM-5.[78] Nitroalkanes can deprotonate to form nitronate anions on γ-alumina, which is a basic catalyst.[46] Yamaguchi observed the aci-anion of nitromethane on γ-alumina.[79] The aci-anion of NM has been observed at room temperature on Na−X [77] and Cs−X[78] and at 373 K on γ-alumina.[79] The aci-anion was converted to a carbonate species upon increasing the temperature to 473 K on MgO[78] and to adducts containing C, N, and O atoms and to a carbonate species above 373 K on γ-alumina.[79] Ross et al. proposed that on γ-alumina the aci-anion of NM isomerizes to an anion of formohydroxamic acid via a three-membered cyclic oxaziridine.[49]

Thus, even though the aci-anion of NM is formed on BaNa−Y, it is expected that in the BaNa−Y environment the lifetime of the aci-anion of NM would be short, and the equilibrium with NM would be expected to favor NM. Presumably, this is because BaNa−Y is not basic enough to significantly stabilize the aci-anion of NM. Moreover, as will be discussed below, dehydration of the aci-anion of NM to give an isocyanate is accelerated by NO_2. In addition, the region from 1600 to 1680 cm^{-1}, in which the C═N vibration of the aci-anion of NM is expected, is dominated by strong absorptions of acetic acid and gas-phase NO_2. Thus, even if there were modest amounts of the aci-anion of NM present, it would be difficult to observe.

As mentioned in Section III. E, the reaction of nitromethane to form CO_2 and ultimately NH_3 is slow on BaNa−Y at 473 K. On the other hand, the reaction of NM was virtually instantaneous after addition of NO_2. This is shown in Figure 11 (spectra a−c) where $^{14}NO_2$ and ^{14}NO form from the reaction of $^{15}NO_2$ with $CH_3{}^{14}NO_2$. It is important to realize that this cannot be due simply to a NO_2 exchange process since NM is consumed as $^{14}NO_2$ is generated. Thus, NO_2 plays an important role in reactions of NM.

Isocyanic acid is observed as an intermediate when NM interacts with BaNa−Y and as a product of the reaction of

SCHEME 3

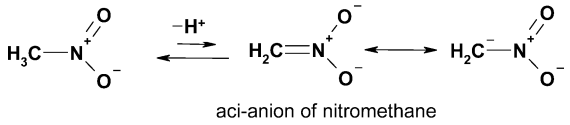

SCHEME 4

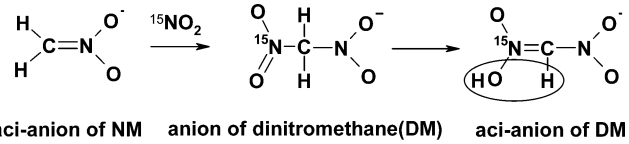

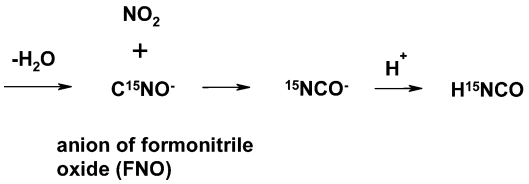

acetaldehyde or acetic acid with NO_2. The fact that both isotopomers of isocyanic acid, HNCO and $H^{15}NCO$, form from the reaction of $^{15}NO_2$ and $CH_3{}^{14}NO_2$ suggests a symmetrical reaction intermediate. The most plausible is a dinitromethane species. If as hypothesized NO_2 reacts with the aci-anion of NM, then the aci-anion of dinitromethane (DNM) ($O_2NCH_2NO_2^-$) could form (see Scheme 4) and would be expected to be stabilized by the ionic environment of BaNa−Y. This process could account for the observed acceleration of the reaction of NM in the presence of NO_2.

Once formed, the aci-anion of DNM can dehydrate while also losing (regenerating) NO_2 to produce CNO^-, the formonitrile-oxide anion (or the fulminate anion). This species can further isomerize and then protonate. The HNCO molecule thus formed can further react with water to give NH_3 and $^{15}NH_3$, respectively.

$$\mathrm{HNCO\ (or\ H^{15}NCO)} + \mathrm{H_2O} \rightarrow \mathrm{NH_3\ (or\ {}^{15}NH_3)} + 2\mathrm{CO_2} \quad (15)$$

If the proposed mechanism in Scheme 4 is operative, $^{15}NO_2$ is consumed, $^{14}NO_2$ is generated, $^{15}NO_2$ is regenerated, and both ^{14}NO and ^{15}NO form since they are in equilibrium with their respective NO_2 isotopomers. This is what is observed. Similarly, just as is experimentally observed (see Figure 12), there should be four N_2O isotopomer products of reactions 15 and 16 since both HNCO and $H^{15}NCO$ are produced using normal nitromethane and ^{15}N labeled $^{15}NO_2$. This is shown in eq 16 which for convenience is balanced using equal amounts of each starting isotopomer.

$$2\mathrm{NH_3} + 2\,{}^{15}\mathrm{NH_3} + 2\mathrm{HNO_3} + 2\mathrm{H^{15}NO_3} \rightarrow \mathrm{N_2O} + \mathrm{N^{15}NO} + {}^{15}\mathrm{NNO} + {}^{15}\mathrm{N^{15}NO} + 8\mathrm{H_2O} \quad (16)$$

The proposed mechanism in Scheme 4 is supported by the fact that in a study by Prins et al.[80] dinitromethane is observed by NMR in several zeolites as a result of the reaction of HNO_3 with acetic anhydride. Further supporting the proposition of a dinitromethane anion intermediate is the fact that a symmetrical $^-O_2NCHNO_2^-$ radical forms when NO_2^- and NM are UV irradiated in 0.5 M NaOH solution.[76] Alkali salts of the DNM anion, which are explosive, have been synthesized.[81,82] Further, the unsaturated character of the aci-anion of NM has been used for trapping various free radical species, such as NO and NO_2.[83]

SCHEME 5

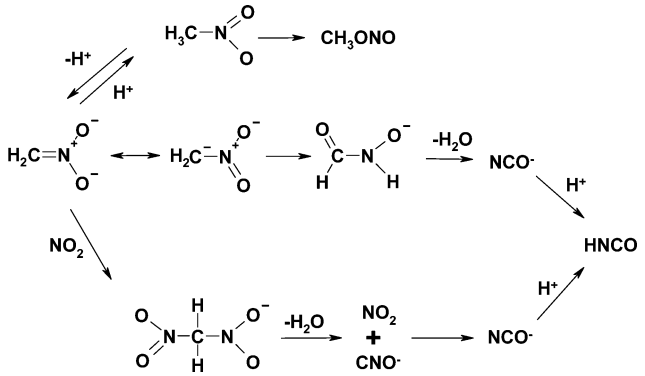

Addition (or trapping) of NO_2 would lead to the anion of dinitromethane. By analogy with what has been calculated for DNM and aci-DNM,[84] it is expected that the dinitromethane anion relatively readily isomerizes to the aci-dinitromethane anion (see Scheme 4) on BaNa−Y.

In the absence of added NO_2, nitromethane can isomerize to either methyl nitrite or form the aci-anion of nitromethane. As shown in Scheme 5, the reaction to form the aci-anion of NM is expected to be reversible while our data indicates that the reaction to form methyl nitrite is not efficiently reversible under experimental conditions. The aci-anion can then isomerize to the anion of formohydroxamic acid. As indicated in Scheme 5, formohydroxamic acid can lose water to form HNCO via a NCO^- intermediate.

With acetaldehyde as the reactant, nitromethane is observed in the gas phase, while with acetic acid as the reactant, NM is not directly observed. Why do these systems behave differently? As shown in Scheme 2, in the presence of NO_2, a direct reaction pathway is proposed that leads to the conversion of acetate ions to the aci-anion of NM. When this anion forms in the presence of NO_2, there is a reaction pathway to form the formohydroxamic acid anion which can then irreversibly dehydrate. This pathway competes with the possible formation of NM from the aci-anion of NM (see Scheme 3). If NM does form, as indicated in section III. E, there is a rapid reaction of the anion of NM with NO_2 to form the anion of DNM. This latter species can decompose to water and CNO^- along with NO_2. One way to look at this process is that NO_2 effectively catalyzes the decomposition of NM.

We do, however, note that there is a literature report of the formation of NM from the homogeneous high-pressure gas-phase reaction of acetic acid with HNO_3.[74] However, under these circumstances, ions would not be expected to be as thermodynamically favorable as in a zeolite environment.

Experimental evidence indicates that acetaldehyde and acetic acid follow the same ionic reaction pathway once the acetate ion is formed. Thus, if we do not observe gas-phase NM with acetic acid as a reactant, NM would not be expected as a product of this reaction pathway with acetaldehyde as a reactant. Though small amounts of gas-phase NM could come from neutralization of ionic intermediates, the most plausible explanation for the formation of observable amounts of gas-phase NM with acetaldehyde as the reactant is that it is produced via another reaction pathway which is open to acetaldehyde but not to acetic acid. Such a pathway is discussed further in Section IV. G.

Despite this statement, there is strong evidence for the involvement of the aci-anion of NM and the anion of DNM in the reaction pathways of both acetic acid and acetaldehyde in the presence of NO_2. As indicated in Schemes 3 and 5, the aci-

anion of NM is expected to be in equilibrium with NM. Thus, adsorbed NM is expected as an intermediate. However, since NO_2 is needed to form NM from either acetic acid or acetaldehyde, and with NO_2 as a reactant there are efficient reaction pathways for the aci-anion of NM, it is not surprising that adsorbed NM is not directly detected in these reaction systems.

F. Subsequent Reactions. Once HNCO forms, the subsequent chemistry of the system is well established. It is well known that HNCO can react with H_2O to give $NH_3 + CO_2$. However, we do not directly observe NH_3 via FTIR spectroscopy under our experimental conditions. The explanation for this is that NH_3 is a weak infrared absorber that is present under steady-state conditions where its concentration is expected to be low. However, we have observed the formation of CO_2 as a result of the reaction of HNCO with water, and NH_3 has been detected via mass spectrometry under similar reaction conditions, albeit for a flowing mixture of acetaldehyde (AA) or NM with NO_2 and H_2O. HNCO also disappears rapidly in the presence of NO_2. However, the details of this latter reaction have not been investigated as part of this study.

Once NH_3 is formed, it can react with HONO to give NH_4NO_2. There is also a report that NH_3 reacts with NO_2 to give N_2.[85] The decomposition of ammonium nitrite to give $N_2 + H_2O$ is a well-known reaction and has been verified in our laboratory to give the indicated products under experimental conditions. In the system under study, HNO_2 can form via the reaction of N_2O_3 with water (which is produced as a reaction product or is added to the system). N_2O_3 is in equilibrium with NO_2 and NO.[16] In fact, we observe N_2O_3 at room temperature when BaNa−Y is exposed to a $NO + O_2$ premix. This sequence of reactions may be one of the factors that lead to an *increase* in the rate of NO_x reduction in the presence of H_2O.

NH_3 can also react with HNO_3 to give N_2O and H_2O as products. The reaction of $NH_3 + HNO_3$ to give N_2O and H_2O has been verified in separate experiments in which BaNa−Y is exposed to only NH_3, HNO_3, and H_2O at 473 K. This reaction is expected to proceed through an ammonium nitrate intermediate.

HCN is also a product of the reaction of AA, acetic acid, or NM with NO_2. The details of the formation and subsequent reactions of HCN are currently under study. There is also an indication that formaldehyde may form when acetaldehyde reacts with NO_2. We plan to investigate whether formaldehyde is a product of the radical channel that will be discussed below, which we believe is also operative when AA is a reactant.

As discussed in section III. D, NO_2 reacts slowly with acetic acid at high acetic acid concentrations. However, at lower acetic acid concentrations a more rapid reaction takes place and several surface-bound intermediates are observed as a result of this reaction that are also observed in the reaction of acetaldehyde with NO_2. On the basis of the position of the absorptions and their isotope shifts, these species are best assigned as surface-bound NCO^- and surface-bound NC^- or CN^- species. CO and CO_2 are also products of these reactions, and as indicated in Section III. C, so is H_2O

Adsorbed NCO^- also disappears in the presence of NO_2. Reference 86 reports the formation of an ONNCO species from the reaction of NCO radial with NO. A similar species could form in our system as a result of the reaction of NCO^- and NO^+, where, as previously discussed, NO^+ is formed by the charge disproportionate reaction upon adsorption of NO_2 on BaNa−Y. Park et al.[87] proposed that surface NCO species adsorbed on a Co−ZSM-5 zeolite interacts with NO_2 leading to N_2, CO_2, and N_2O, whereas NCO was stable up to 723 K in the presence of NO or O_2. Kung et al.[88] reported that N_2 was formed when NO was pulsed over a $Cu-ZrO_2$ catalyst with adsorbed CN and NCO species.

SCHEME 6

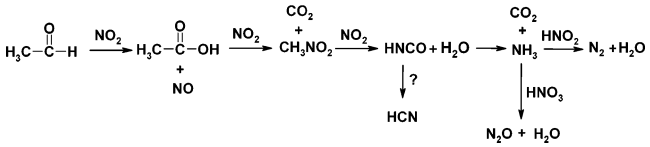

The CO/CO_2 ration was measured with both AA and acetic acid as starting materials. Much more CO is observed as a reaction product (CO_2/CO ratio of ∼2:1) when the starting material is AA than with acetic acid, where the ratio is ∼24:1. In these studies, calibration experiments were preformed with known amounts of CO and CO_2 so that relative band intensities of CO and CO_2 could be converted to relative concentrations. It was also verified that CO was not oxidized to CO_2 under reaction conditions. Additionally, methyl alcohol is observed as a reaction product when acetaldehyde is a reactant, but it is not observed with acetic acid as a reactant. As indicated above, there is also evidence that formaldehyde and gas-phase NM are products of the reaction of acetaldehyde and NO_2. The change in the CO_2/CO ratio, along with the observation of new products, implies that there is an additional reaction pathway for the reaction of AA with NO_2 versus acetic acid with NO_2. That pathway will be commented on further below.

In summary, the results of this study show that a predominant pathway for the reduction of NO_2 with acetaldehyde to form ammonia involve the following key reactants, products, and intermediates:

$$CH_3CHO \rightarrow CH_3COO^- \rightarrow CH_2NO_2^- \rightarrow O_2NCH_2NO_2^- \rightarrow HNCO \rightarrow NH_3 \quad (17)$$

NO_2 is the reaction partner in the first four of these steps, whereas H_2O reacts with HNCO to form $NH_3 + CO_2$ in the final step. The neutral species involved in the overall mechanism as reactants and products are shown in Scheme 6.

G. A Second Reaction Pathway for Acetaldehyde Oxidation. The reaction sequence shown in eq 17 involves an acetate ion. If this were the only reaction pathway operative, it should not matter whether this acetate ion formed from acetaldehyde or acetic acid, and the same reaction products would be expected to be present in a common ratio. However, this is not what is seen. The CO/CO_2 ratio is much higher with acetaldehyde than with acetic acid as the reactant.

This change in CO/CO_2 ratio could be a consequence of aldol condensation to crotonaldehyde, followed by its polymerization and reaction of the thus formed carbonaceous deposit with water vapor. Chen et al.[89] found that the CO/CO_2 ratio resulting from NO_x reduction over Fe/MFI catalysts was much higher for feeds containing water vapor than for a dry feed. These authors showed that a carbonaceous deposit was indeed formed and re-volatilized by water vapor with CO being a major gaseous product. However, we have found that the CO/CO_2 does not change significantly on addition of 2.0 Torr of H_2O to the reaction cell. This result implies that a mechanism analogous to what Chen et al. observed is not significant in our reaction system.

Additionally, methanol is detected in the reaction product mix with acetaldehyde as the reductant indicating a second pathway for the reaction of acetaldehyde. This pathway could involve

radicals produced in the reaction of NO_2 with acetaldehyde. A plausible pathway that is compatible with existing data would start with abstraction of the carbonyl H of acetaldehyde by NO_2:

$$CH_3C(O)H + NO_2 \rightarrow CH_3CO + HNO_2 \qquad (18)$$

The C−H bond dissociation energies of gas-phase acetaldehyde has been experimentally determined as 89.3 kcal/mol for the carbonyl hydrogen and 95.92 kcal/mol at 0 K for the methyl hydrogens. Thus, in the gas phase reaction 18 is endothermic by only ∼8 kcal/mol.[90]

CH_3CO radicals are well-known species. They have been formed by abstraction of hydrogen from acetaldehyde with chlorine atoms and have been detected using matrix isolation.[38] Acetyl radicals have also been produced in a Na−Y zeolite by photodissociation of 1-naphthyl acetate and pinacolone and these radicals have reported lifetimes of 71 (1-naphthyl acetate) and 315 s (pinacolone) at room temperature.[91] The observations of these long lifetimes for radicals in Na−Y[91] and Na−X [92] implies that radicals created in the same supercage separate from the point at which they were generated and that at least one of these species moves though the zeolite to find a reaction partner.

The acetyl radical was detected at 2125 cm^{-1},[91] which is a large blue shift relative to the CH_3CO radical in hexane solution (1864 cm^{-1}). The authors of ref 91 attributed the large blue shift to the interaction of the radical with Na^+ cations in Na−Y. Such an interaction could stabilize the acetyl radicals on the surface of the BaNa−Y zeolite. Consistent with this statement, our data demonstrates that HONO can interact with the zeolite surface. Both of these interactions could shift the reaction thermochemistry and potentially make reaction 18 exothermic.

There are several possibilities for the fate of the acetyl radical in the system under study. One is reaction with HNO_2 to form acetic acid and NO as shown in reaction 19.

$$CH_3CO + HNO_2 \rightarrow CH_3C(O)OH + NO \qquad (19)$$

Additionally, methyl radicals and CO could be formed by dissociation of the acetyl radical.

$$CH_3CO \rightarrow CH_3 + CO \qquad (20)$$

Acetyl radicals could also react with NO_2 and O_2 in reactions 21 and 22.

$$CH_3CO + NO_2 \rightarrow CH_3ONO + CO \qquad (21)$$

Each of the above reactions (20 and 21) leads to CO as a product, which is consistent with a greater CO/CO_2 ratio with acetaldehyde versus acetic acid as the reductant. Also, gas-phase NM is observed as a result of the reaction of acetaldehyde + NO_2 but not when acetic acid reacts with NO_2.

$$CH_3CO + O_2 \rightarrow CH_3O_2 + CO \qquad (22)$$

Acetyl radicals could also produce acetoxy radicals upon reaction with NO_2 (reaction 23). The acetoxy radicals are quite unstable (dissociation energy for reaction 24 is −10 kcal/mol) and rapidly (lifetime = $\sim 10^{-10}$ s) decompose into methyl radicals and carbon dioxide.[93]

$$CH_3CO + NO_2 \rightarrow CH_3CO_2 + NO \qquad (23)$$

$$CH_3CO_2 \rightarrow CH_3 + CO_2 \qquad (24)$$

Though the reactions presented in this section are mostly speculation, the "second" reaction pathway for acetaldehyde is clearly of interest for future investigations.

H. Role of Surface Nitrate in Hydrocarbon Oxidation Reactions. There is much discussion in the literature of the involvement of surface nitrates in hydrocarbon oxidation reactions. Though a detailed mechanism was not provided, there have been several reports that surface nitrates are responsible for the oxidation of propene on alumina,[94] HNa−mordenite,[27] Ba−Y,[20] and $Pt/BaCl_2/SiO_2$.[30] Shimizu et al. reported on the role of surface nitrates in NO_x SCR with propene over alumina at 573 K.[94] They asserted that surface nitrate is responsible for the oxidation of propene to acetate and acetate to CO and CO_2. In similar work, it was reported that the concentration of NO_3^- decreased by reaction with propene on HNa−mordenite at 573 K to about 50% of the initial amount after 1 h and by ∼80% after 4 h.[27] Sedlmair reported that surface nitrate and nitrite species were potentially responsible for oxidation of propene to carboxylic acid and isocyanates on Ba−Y.[20] Coronado et al. found that $Ba(NO_3)_2$ species were formed upon introducing NO_2 onto $Pt/BaCl_2/SiO_2$ and they proposed that propene reacted with a NO_x species which is produced from the decomposition of the $Ba(NO_3)_2$.[30]

As alluded to above, we have observed two different classes of surface nitrates. One species markedly decreases in intensity when acetic acid or acetaldehyde is introduced into the system. This nitrate species participates in a reaction with acetic acid and acetaldehyde and can be largely removed simply by evacuation of the cell. The other species is sufficiently strongly bound that it remains after evacuation of the cell and is effectively unreactive in the presence of acetic acid or acetaldehyde.

V. Conclusions

A crucial step for most or all deNO_x catalysts is formation of ammonium nitrite, NH_4NO_2. This compound swiftly decomposes to $N_2 + H_2O$ near 100 °C. It is formed from HONO and NH_3, both of which are produced in situ over the catalyst. Detailed studies of the Fe/MFI system, using isotopic labeling, have shown that the ultimate N_2 molecules each consist of one N atom from HONO and the other from NH_3.[3,12] The overall conversion is highest for a NO/NO_2 ratio = 1, because at this ratio HONO reaches maximum values because of the gaseous equilibria: $NO + NO_2 = N_2O_3$ and $H_2O + N_2O_3 = 2HONO$.

Perhaps the most significant result of this study is that reactions that take place on the BaNa−Y zeolite can effect changes in the oxidation state of N in going from NO_x to N_2 without the benefit of a transition metal. Our results show that this is achieved in a multistep mechanism. Acetaldehyde reacts with NO_2 to first form acetate ions and subsequently the aci-anion of nitromethane. The aci-anion of nitromethane can dehydrate to form isocyanic acid, HNCO, in a process that is strongly accelerated by NO_2. We propose a mechanism in which NO_2 reacts with the aci-anion of CH_3NO_2, which is stabilized in the ionic environment of the zeolite forming the proposed $O_2NCH_2NO_2^-$ anion intermediate. Such an intermediate is consistent with the observation of $^{14}NO_2$ formation and the production of both isotopomers of HNCO when nitromethane reacts with $^{15}NO_2$. As expected for an $O_2NCH_2NO_2^-$ intermediate, and as illustrated in reaction 16, all four isotopomers of N_2O are observed. Formation of nitromethane is observed in the reaction of acetaldehyde + NO_2. Nitromethane could come from the neutralization of an ionic precursor or via the radical channel discussed in Section IV. G where NM could form via reaction of methyl radicals and NO_2.

At 473 K, $O_2NCH_2NO_2^-$ swiftly loses NO_2 and H_2O yielding the formonitrile oxide anion, CNO^-, which can react with a proton to form HNCO. The next step, formation of $NH_3 + CO_2$ from $HNCO + H_2O$, is basically the same as reported previously by Poignant et al.[67] for Cu/MFI.

Summarizing, ammonia is thus formed by the schematic sequence shown in eq 17:

$$CH_3CHO \rightarrow CH_3COO^- \rightarrow CH_2NO_2^- \rightarrow O_2NCH_2NO_2^- \rightarrow CNO^- \rightarrow HNCO \rightarrow NH_3$$

with NO_2 being the reaction partner in the first three steps, a proton is added in the fifth step, and H_2O is the co-reactant in step 6. In the absence of NO_2, isocyanic acid can react to form cyanamide and cyanuric acid.

In this chemistry, the high electric field strength in zeolite cavities favors charged intermediates, including the aci-anion of nitromethane. Another manifestation of this environment is that N_2O_4, the dimer of NO_2, is chemisorbed as NO^+ and NO_3^-. This heterolytic dissociation dissipates the twofold charge of Ba^{2+} forming two monopositive entities, $[Ba-NO_3]^+$ and NO^+, which can each migrate to positions near the immobile loci of the negative charge in the zeolite lattice. With zeolites, such dissipation of the charge of multivalent cations can enhance the Coulomb energy.

Acetaldehyde also undergoes an aldol condensation over BaNa−Y. If crotonaldehyde is formed, it can polymerize to molecules that are large enough to block channels or sites in the zeolites. However, the addition of NO_2 opens up a reaction pathway for acetaldehyde that effectively competes with the aldol condensation process.

The major reaction channel outlined above is also followed by acetic acid and results in a very high CO_2/CO ratio ($>20:1$). The reaction of either acetic acid or acetaldehyde with NO_2 gives a similar set of products except that the CO to CO_2 ratio is relatively higher with acetaldehyde as a reactant *and* methanol and gas-phase NM are observed as reaction products with acetaldehyde as a reactant but are not observed when acetic acid is the reductant. These observations suggest that a parallel channel exists for acetaldehyde that could involve free radicals. Such a path would likely be initiated by NO_2 abstracting a H atom from acetaldehyde. The resulting acetyl radical can dissociate to CO and a methyl radical. The methyl radical can participate in subsequent reactions.

Acknowledgment. This work was supported by the EMSI program of the National Science Foundation and the U.S. Department of Energy, Office of Science (CHE-9810378) and by the Chemical Sciences, Geosciences and Biosciences Division, Office of Basic Energy Sciences, Office of Science, U.S. Department of Energy (DE-FG02-03-ER15457), at the Northwestern University Institute for Environmental Catalysis. We also thank Professors John Yates and Vicki Grassian for providing very helpful information dealing with the design and construction of the "wire gauze" reactor used in these experiments.

References and Notes

(1) Chen. H. Y.; Sachtler, W. M. H. *Catal. Today* **1998**, *42*, 73.
(2) Roberge, D.; Raj. A.; Kaliaguine, S.; Trong On, D.; Inui, I. T. *Appl. Catal., B* **1996**, *10*, L237.
(3) Sun, Q.; Gao, Z. X.; Chen, H. Y.; Sachtler, W. M. H. *J. Catal.* **2001**, *201*, 89.
(4) Kung, H. H. *Stud. Surf. Sci. Catal.* **1989**, *45*, 169.
(5) Sachtler, W. M. H. *Recueil Trav. Chim. Pays-Bas* **1963**, *82*, 243.
(6) Crasseli, R. K.; Burington, J. D. *Adv. Catal.* **1981**, *30*, 133.
(7) Mars, P.; van Krevelen, D. W. *Chem. Eng. Sci. (Spec. Suppl.)* **1954**, *3*, 41.
(8) Iwamoto, M.; Hamada, H. *Catal. Today* **1991**, *10*, 57.
(9) Iwamoto, M. In *Zeolites and Related Microporous Materials: State of the Art*; Weitkamp, J., Karge, H. G., Pfeifer, H., Hölderich, W., Eds.; Proceedings of the 10th IZC; Elsevier: Garmisch-Partenkirchen, Germany, 1994; Part B, pp 1395−1410.
(10) Chen, H. Y.; Voskoboinikov, T.; Sachtler, W. M. H. *J. Catal.* **1998**, *180*, 171.
(11) Chen, H. Y.; Voskoboinikov, T.; Sachtler, W. M. H. *J. Catal.* **1999**, *186*, 91.
(12) Sun, Q.; Gao, Z. X.; Wen, B.; Sachtler, W. M. H. *Catal. Lett.* **2002**, *78*, 1.
(13) (a) Lide, D. R. et al. In *Handbook of Chemistry and Physics*, 83th ed.; CRC Press: Boca Raton, FL, 2002. (b) Greenwood, N. N.; Earnshan, A.; *Chemistry of the Elements*; Pergamon Press: New York, 1984; p 471.
(14) Satsuma, A.; Cowan, A. D.; Cant, B. W.; Trimm, D. L. *J. Catal.* **1999**, *181*, 165.
(15) Panov, G.; Tonkyn, R. G.; Balmer, M. L.; Peden, C. H. F. *Society of Automotive Engineering* **2001**, 01−3513.
(16) Wen, B.; Yeom, Y. H.; Weitz, E.; Sachtler, W. M. H. *Appl. Catal., B* **2004**, *48*, 125.
(17) Basu, P.; Ballinger, T. H.; Yates, J. T. *Rev. Sci. Instrum.* **1988**, *59*, 1321.
(18) Greenwood, N. N.; Earnshan, A. *Chemistry of the Elements*; Pergamon Press: New York, 1984; p 522.
(19) Bentrup, U.; Bruckner, A.; Richter, M.; Fricke, R. *Appl. Catal., B* **2001**, *32*, 229.
(20) Sedlmair, C.; Gil, B.; Sechan, K.; Jentys, A.; Lercher, J. A. *Phys. Chem. Chem. Phys.* **2003**, *5*, 1897.
(21) Ivanova, E.; Hadjiivanov, K.; Klissurski, D.; Bevilacqua, M.; Armaroli, T.; Busca, G. *Microporous Mesoporous Mater.* **2001**, *46*, 299.
(22) Szanyi, J.; Kwak, J. H.; Moline, R. A.; Peden, C. submitted to *Phys. Chem. Chem. Phys.*
(23) Hertzberg, G. *Molecular Spectra and Molecular Structure*; Van Nostrand: New York, 1945, Vol II.
(24) Hadjiivanov, K. I. *Catal. Rev. Sci. Eng.* **2000**, *42*, 71.
(25) Henriques, C.; Marie, O.; Thibault-Starzyk, F.; Lavalley, J. C. *Microporous Mesoporous Mater.* **2001**, *50*, 167.
(26) Chao, C. C.; Lunsford, J. H. *J. Am. Chem. Soc.* **1971**, *93*, 71.
(27) Satsuma, A.; Enjoji, T.; Shimizu, K. I.; Sato, K.; Yoshida, H.; Hattori, T. *J. Chem. Soc., Faraday Trans.* **1998**, *94*, 301.
(28) Monticelli, O.; Loenders, R.; Jacobs, P. A.; Martens, J. A. *Appl. Catal., B* **1999**, *21*, 215.
(29) Thomas, K. J.; Ramamurthy V. *Langmuir* **1998**, *14*, 6687.
(30) Cornado, J. M.; Anderson, J. A. *J. Mol. Catal. A* **1999**, *138*, 83.
(31) Prinetto, F.; Ghiotti, G.; Nova, I.; Lietti, L.; Tronconi, E.; Forzatti, P. *J. Phys. Chem. B* **2001**, *105*, 12732.
(32) Xu, C.; Koel, B. E. *J. Chem. Phys.* **1995**, *102*, 8158.
(33) Jeong, M. S.; Frei, H. *J. Mol. Catal. A: Chemical* **2000**, *156*, 245.
(34) Oelichmann, H. J.; Bougeard, D.; Schrader, B. *J. Mol. Struct.* **1981**, *77*, 179.
(35) Shimanouchi, T. *Tables of Molecular Vibrational Frequencies Consolidated*; National Bureau of Standards (Washington, DC), 1972; Vol. 1, pp 1−160.
(36) Silvestre-Albero, J.; Sepulveda-Escribano, A.; Rodriguez-Reinoso, F.; Anderson, J. A. *Phys. Chem. Chem. Phys.* **2003**, *5*, 208.
(37) Yeom, Y. H.; Kim, Y.; Seff, K. *J. Phys. Chem. B* **1997**, *101*, 5314.
(38) Couvas, J. W.; Jones, R. H.; Thomas, J. M.; Smith, B. J. *Adv. Mater.* **1990**, *2*, 181.
(39) Martra, G.; Ocule, R.; Marchese, L.; Centi, G.; Coluccia, S. *Catal. Today* **2002**, *73*, 83.
(40) Physical Sciences Information Gateway, http://www.psigate.ac.uk/newsite/reference/chemdata/11.html.
(41) (a) Mielke, Z.; Adrews, L. *J. Phys. Chem.* **1990**, *94*, 3519. (b) Lowenthal, M. S.; Khama, R. K.; Moore, M. H. *Spectrochim. Acta, Part A* **2000**, *58*, 73.
(42) (a) Cant, N. W.; Liu, I. O. Y. *Catal. Today* **2000**, *63*, 133. (b) Lombardo, E. A.; Sill, G. A.; d'Itri, J. L.; Hall, W. K. *J. Catal.* **1997**, *173*, 440.
(43) Cant, N. W.; Chambers, D. C.; Cowan, A. D.; Liu, I. O. Y.; Satsuma, A. *Top. Catal.* **2000**, *10*, 13.
(44) Matyshak, V. A.; Krylov, O. V. *Catal. Today* **1995**, *25*, 1.
(45) Schriver, A.; Schriver-Mazzuoli, L.; Chaquin, P.; Bahou, M. *J. Phys. Chem. A* **1999**, *103*, 2624.
(46) Angevaare, P. A. J. M. Ph.D. Thesis, "Surface Chemistry of Oxygen Containing Compounds on Oxides", State University of Leiden, Netherlands, 1991.
(47) Yeom, Y. H.; Frei, H. *J. Phys. Chem. A* **2002**, *106*, 3350.
(48) Hu, W. F.; He, T. J.; Chen, D. M.; Liu, F. C. *J. Phys. Chem. A* **2002**, *106*, 7294.
(49) Zuzaniuk, V.; Meunier, F.; Ross, J. R. H. *J. Catal.* **2001**, *202*, 340.

(50) Nguyen, M. T.; Le, H. T.; Hajgato, B.; Veszpremi, T.; Lin, M. C. *J. Phys. Chem. A* **2003**, *107*, 4286.
(51) Rook, F.; Jacox, M. *J. Mol. Spectrosc.* **1982**, *93*, 101.
(52) Fieberg, J. E.; White, J. M. *J. Vac. Sci. Technol., A* **1997**, *15*, 1674.
(53) Bares, A. J.; Hallem, H. E.; Waring S.; Armstrong, J. R. *J. Chem. Soc., Faraday Trans. 2* **1976**, 1.
(54) Saldyka, M.; Mielke, Z. *Chem. Phys. Lett.* **2003**, *371*, 713.
(55) From FT-IR spectra of cyanamide which is supplied by Sigma-Aldrich Co.
(56) Mindiola, D. J.; Tsai, Y. C.; Hara, R.; Chen, Q.; Meyer, K.; Cummins, C. C. *Chem. Commun.* **2001**, *1*, 125.
(57) Fisher, G.; Geith, J.; Klapotke, T. M.; Krumm, B. *Z. Naturforsch., B* **2002**, *57*, 19.
(58) (a) Tordini, F.; Bencini, A.; Bruschi, M.; Gioia, L. D.; Zampella, G.; Fantucci, P. *J. Phys. Chem. A* **2003**, *107*, 1188. (b) Belsky, A. J.; Brill, T. B. *J. Phys. Chem. A* **1998**, *102*, 4509.
(59) Feng, W. L.; Wang, Y.; Zhang, S. W. *J. Mol. Struct.* **1995**, *342*, 147.
(60) He, Y.; Liu, X.; Lin, M. C. *Int. J. Chem. Kint.* **1991**, *23*, 1129.
(61) Baldinozzi, G.; Malinowska, B.; Rakib, M.; Durand, G. *J. Mater. Chem.* **2002**, *12*, 268.
(62) Becker, M.; Jansen, M.; Lieb, A.; Milius, W.; Schnick, W. *Z. Anorg. Allg. Chem.* **1998**, *624*, 113.
(63) Schaber, P. M.; Colson, J.; Higgins, S.; Dietz, E.; Thielen, D.; Anspach, B.; Brauer, J. *Am. Lab.* **1999**, *31*, 13.
(64) Lapinski, A.; Spangel-Larsen, J.; Waluk, J.; Radziszewski, J. G. *J. Chem. Phys.* **2001**, *115*, 1757.
(65) (a) Miller, J. A.; Bowman, C. T. *Int. J. Chem. Kinet.* **1991**, *23*, 289. (b) He, Y.; Liu, X.; Lin, M. C.; Melius, C. F. *Int. J. Chem. Kinet.* **1993**, *25*, 845.
(66) Siebers, D. L.; Caton, J. A. *Combust. Flame* **1990**, *79*, 31.
(67) Poignant, F.; Saussey, J.; Lavalley, J. C.; Mabilon, G. *Chem. Commun.* **1995**, 89.
(68) Liu, I. O. Y.; Cant, N. W.; Haynes, B. S.; Nelson, P. F. *J. Catal.* **2001**, *203*, 487.
(69) (a) Kleeman, M.; Elsemer, M.; Koebel, M.; Wokaum, A. *Ind. Eng. Chem. Res.* **2000**, *39*, 4120. (b) Lister, M. W. *Canadian J. Chem.* **1955**, *33*, 426.
(70) (a) Madia, G.; Koebel, M.; Elsener M.; Wokaun, A. *Ind. Eng. Chem. Res.* **2002**, *41*, 3512. (b) Koebel, M.; Elsener M.; Madia, G. *Ind. Eng. Chem. Res.* **2001**, *40*, 52.
(71) Dumitriu, E.; Hulea, V.; Fechete, I.; Auroux, A.; Lacaze, J. F.; Guimon, C. *Microporous Mesoporous Mater.* **2001**, *43*, 341.
(72) Wenthold, P. G.; Squires, R. R. *J. Am. Chem. Soc.* **1994**, *116*, 11890.
(73) Ashworth, B.; Davis, M. J.; Gilbert, B. C.; Norman, R. O. C. *J. Chem. Soc., Perkin Trans. 2* **1983**, 1755.
(74) (a) Mari, R.; Nancy, V. L.; Quibel, J.; Laffitte, M. U.S. Patent 4,992,603, 1991. (b) Sherwin, M. B. U.S. Patent 4,476,336, 1984.
(75) Wang, S. C. P.; Sherwin, M. B. U.S. Patent 4,524,226, 1985.
(76) Bilski, P.; Chignell, C. F.; Szychlinski, J.; Borkowaski, A.; Oleksy, E.; Reszka, K. *J. Am. Chem. Soc.* **1992**, *114*, 549.
(77) Ellison, E. H.; Thomas, J. K. *Langmuir* **2001**, *17*, 2446.
(78) Kheir, A. A.; Haw, J. F. *J. Am. Chem. Soc.* **1994**, *116*, 817.
(79) Yamaguchi, M. *J. Chem. Soc., Faraday Trans.* **1997**, *93*, 3581.
(80) Haouas, M.; Bernasconi, S.; Kogelbauer, A.; Prins, R. *Phys. Chem. Chem. Phys.* **2001**, *3*, 5067.
(81) (a) Grakauskas, V.; Guest, A. M. *J. Org. Chem.* **1978**, *43*, 3485. (b) Langlet, A.; Latypov, N. V.; Wellmar, U.; Bemm, U.; Goede, P. *J. Org. Chem.* **2002**, *67*, 7833.
(82) Singh, K. *Spectrochim. Acta* **1967**, *23*, 1089
(83) Bilski, P.; Reszka, K.; Chignell, C. F. *J. Am. Chem. Soc.* **1994**, *116*, 9883.
(84) (a) Khrapkovskii, G. M.; Shamov, A. G.; Shamov, G. A.; Shlyapochnikov, V. A. *Russ. Chem. Bull. Int. Ed.* **2001**, *50*, 952. (b) Khrapkovskii, G. M.; Shamov, A. G.; Shamov, G. A.; Shlyapochnikov, V. A. *Meendeleev Commun.* **1997**, *7*, 169.
(85) Stevenson, S. A.; Vartuli, J. C. *J. Catal.* **2002**, *208*, 100.
(86) Cooper, W. F.; Hershberger, J. F. *J. Phys. Chem.* **1992**, *96*, 771.
(87) Goryashenko, S. S.; Park, Y. K.; Kim, D. S.; Park, S. E. *Res. Chem. Intermed.* **1998**, *24*, 933.
(88) Li, C.; Bethke, K.; Kung, H.; Kung, M. C. *J. Chem. Soc., Chem. Commun.* **1995**, 813.
(89) Chen, H. Y.; Sachtler, W. M. H. *Catal. Today* **1998**, *42*, 73.
(90) Slagle, I. R.; Gutman, D. *J. Am. Chem. Soc.* **1982**, *104*, 4741.
(91) Vasenkov, S.; Frei, H. *J. Phys. Chem. A* **2000**, *104*, 4327.
(92) Johnston, L. J.; Scaiano, J. C.; Shi, J. L.; Siebrand, W.; Zerbetto, F. *J. Phys. Chem.* **1991**, *95*, 10018.
(93) Nimlos, M. R.; Soderquist, J. A.; Ellison, G. B. *J. Am. Chem. Soc.* **1989**, *111*, 7675.
(94) Shimizu, K. I.; Kawabata, H.; Satsuma, A.; Hattori, T. *J. Phys. Chem. B* **1999**, *103*, 5240.
(95) Su, H.; Kong, F.; Chen, B.; Huang, M. B.; Liu, Y. *J. Chem. Phys.* **2000**, *113*, 1885.
(96) Quapp, W.; Albert, S.; Winnewisser, B. P.; Winnewisser, M. *J. Mol. Spectrosc.* **1993**, *160*, 540.
(97) Pavlosky, M. A.; Larrabee, J. A. *J. Am. Chem. Soc.* **1988**, *110*, 5349.
(98) Morrow, B. A.; Cody, I. A. *J. Chem. Soc., Faraday Trans.* 1 **1975**, *71*, 1021.
(99) Pinchas, S.; Laulicht, I. *Infrared Spectra of Labeled Compounds*; Academic Press: New York, 1971.